LASER INTERFEROMETER GRAVITATIONAL WAVE OBSERVATORY

LIGO Laboratory / LIGO Scientific Collaboration

LIGO-T0900496-v4 *Advanced LIGO UK* 1st March 2011

Advanced LIGO BOSEM Noise Measurement Report

Stuart Aston

Distribution of this document:
Inform aligo_sus

This is an internal working note
of the Advanced LIGO Project, prepared by members of the UK team.

Institute for Gravitational Research
University of Glasgow
Phone +44 (0) 141 330 5884
Fax +44 (0) 141 330 6833
E-mail k.strain@physics.gla.ac.uk

School of Physics and Astronomy
University of Birmingham
Phone +44 (0) 121 414 6447
Fax +44 (0) 121 414 3722
E-mail av@star.sr.bham.ac.uk

Engineering Department
CCLRC Rutherford Appleton Laboratory
Phone +44 (0) 1235 445 297
Fax +44 (0) 1235 445 843
E-mail J.Greenhalgh@rl.ac.uk

Department of Physics
University of Strathclyde
Phone +44 (0) 1411 548 3360
Fax +44 (0) 141 552 2891
E-mail N.Lockerbie@phys.strath.ac.uk

http://www.ligo.caltech.edu/

http://www.physics.gla.ac.uk/igr/sus/

http://www.sr.bham.ac.uk/research/gravity/rh,d,2.html

http://www.eng-external.rl.ac.uk/advligo/papers_public/ALUK_Homepage.htm

1 Introduction and Scope *4*
1.1 Version History **4**
1.2 Document Organization **4**
1.3 System Overview **4**
1.4 Acronym List **5**
1.5 References **5**
2 BOSEM Noise Measurements *6*
2.1 Test Set-up **6**
2.2 Test Procedure **7**
2.3 Test Results **9**
2.4 Discussion **9**
3 NPOSEM Noise Measurements *10*
3.1 Test Set-up **10**
3.2 Test Procedure **10**
3.3 Test Results **11**
3.4 Discussion **11**
4 Study into the Source of Excess Noise *12*
4.1 Reproducibility **13**
4.1.1 Test Set-up 13
4.1.2 Test Procedure 14
4.1.3 Test Results 14
4.1.4 Discussion 14
4.2 Flexi-circuit Investigation **15**
4.2.1 Test Set-up 15
4.2.2 Test Procedure 15
4.2.3 Test Results 16
4.2.4 Discussion 16
4.3 Sensor Investigation **17**
4.3.1 Test Set-up 17
4.3.2 Test Procedure 17
4.3.3 Test Results 17
4.3.4 Discussion 19
4.4 Open-light Investigation **19**
4.4.1 Test Set-up 19
4.4.2 Test Procedure 19
4.4.3 Test Results 19
4.4.4 Discussion 21

4.5 Axial Symmetry Investigation 21
4.5.1 Test Set-up 21
4.5.2 Test Procedure 21
4.5.3 Test Results 22
4.5.4 Discussion 22
4.6 Thermal Environment 22
4.6.1 Test Set-up 23
4.6.2 Test Procedure 23
4.6.3 Test Results 23
4.6.4 Discussion 24
4.7 Lens Geometry Investigation 24
4.7.1 Test Set-up 24
4.7.2 Test Procedure 24
4.7.3 Test Results 25
4.7.4 Discussion 25
5 IRLED Screening 26
5.1 Test Set-up 26
5.2 Test Procedure 26
5.3 Production Batch IRLEDs 27
5.4 Verification of IRLED Screening 28
5.5 COTS Batch IRLED Results 29
5.6 Verification of IRLED Screening 30
5.7 Burn-in Investigation 31
5.8 IRLED Package Dissection 32
5.9 Alternative IRLED (Vishay TSTS7100) 34
6 Conclusions and First 50 Full Characterization Results 37
7 Production BOSEM Full Characterization Results 43
8 Production BOSEM Automated Test Equipment Results 50
9 APPENDIX A – IRLED Screening Procedure – V3 (UoB Internal) 53

1 Introduction and Scope

Production of the required number of BOSEMs was completed at the end of September 09 and these units were ready to ship. However, we received a request from US colleagues to provide noise performance plots for each individual unit before commencing with the shipment. This was not part of the production plan as was signed-off by the Review Committee [1], but we agreed to perform noise measurements on a random sample of units.

Originally only a small number of these noise measurements were made on bench-top and "Noise Prototype" units both at Birmingham and Strathclyde, which raised no concerns. This document outlines our findings for the characterization of the production articles.

1.1 Version History

Rev. v1 - Initial release. 24th November 2009 (SMA)

Rev. v2 - Updated to include IRLED Burn-in tests. Revised section 6. 8th December 2009 (SMA).

Rev. v3 - Updated figures 12, 13, 14, 18, 20 & 22. Added sections 5.8 & 5.9. 23rd June 2010 (SMA). Revised sections 1 and 6. Minor corrections throughout. 6th September 2010 (SMA).

Rev. v4 - Added final BOSEM characterisation plots. Added some analysis of ATE results, PD current distribution etc. Updated references. Added Section 7 and 8. 1st March 2011 (SMA).

1.2 Document Organization

The document is organized as follows:-

- Section 2, Characterization of BOSEMs
- Section 3, Characterization of NPOSEMs
- Section 4, Investigation into the Source of Excess Noise
- Section 5, IRLED Screening
- Section 6, Conclusions and First 50 Characterization Results
- Section 7, Production BOSEM Full Characterization Results
- Section 8, Production BOSEM Automated Test Equipment Results

1.3 System Overview

A detailed understanding of the design and operation of the BOSEM can be obtained from the "BOSEM Design Document and Test Report" [2].

An overview of the key components of the BSOEM can be obtained by observing diagrams available in the "BOSEM Assembly Specification" [3].

1.4 Acronym List

ALUK	Advanced LIGO UK
ATE	Automated Test Equipment
BOSEM	Birmingham OSEM
COTS	Commercial Off-The-Shelf
DVM	Digital Volt Meter
IOSEM	Initial LIGO OSEM
IRLED	Infrared Light Emitting Diode
LIGO	Laser Interferometer Gravitational Wave Observatory
NPOSEM	Noise Prototype OSEM
OSEM	Optical Shadow sensor and Electro-Magnetic actuator
PD	Photodiode
PEEK	Polyether ether ketone
PFA	Perfluoroalkoxy fluoropolymer (Du Pont)
PSU	Power Supply Unit
SUS	Suspensions Working Group
TBC	To Be Confirmed
TBD	To Be Determined
TO	Transistor Outline
UHV	Ultra High Vacuum
UK	United Kingdom
UoB	University of Birmingham
US	United States of America

1.5 References

(1) B.Bland *et al*, “Report on BOSEM FDR and FRR”, L080022-00-E

(2) S.Aston, “BOSEM Design Document and Test Report”, T050111-04-K

(3) S.Aston and D.Lodhia, “BOSEM Assembly Specification”, T060233-03-K

(4) S.Aston, “Noise Prototype OSEM Design Change Log”, T060137-01-K

(5) D. Ursutiu and B. Jones “Low-frequency noise used as a lifetime test of LEDs”.

(6) N. Lockerbie, “OP232 IR LED + SMD2420 Photodiode: Output vs Flag Displacement”, T040178-00

2 BOSEM Noise Measurements

The production BOSEMs have been assembled in accordance with the assembly specification [3]. To enable us to make noise measurements on UHV-clean units they are required to be relocated to one of our laboratories, which is not a UHV-clean environment. We therefore adopted the best handling practices feasible throughout the duration of these tests in an effort to maintain UHV-compliance of the final articles.

After the completion of the tests the sample BOSEMs are returned to the clean-room facility, where they will undergo the final stage cleaning process (again), prior to be packaged ready for shipping to the US. Upon arrival at Caltech they will undergo the final stage cleaning and bake-out with the rest of the batch of BOSEMs.

2.1 Test Set-up

We wish to simulate as near as possible, the real world operation of the BOSEM. To provide an extensive end-to-end test of the BOSEM a spare Satellite Box has been used to drive the IRLED and provide front-end amplification for the PDs. The BOSEM harness has also been fabricated as per the current design specification (twisted pairs, with overall copper shield and PEEK braid). Table 1 provides a list of test equipment used throughout the duration of these tests.

Device Type	Manufacturer	Model	Serial Number
Digital Signal Analyzer	Agilent	35670A	MY42507469
Low Noise Preamplifier	SRS	SR560	82111
DVM	Beckman Industrial	T120B	80429020
PSU	Farnell	LT30-2	010269
IRLED driver, PD front-end	UoB	Satellite Box	#007

Table 1. List of Test Equipment.

The BOSEM is mounted using bespoke fixtures to a passively damped optical bench. A 3mm diameter flag is attached to a translation stage which allows it to be translated along the sensing axis of the BOSEM. Figure 1 shows the BOSEM ready to be characterized, mounted on the test fixtures, also shown is an early prototype Satellite Box.

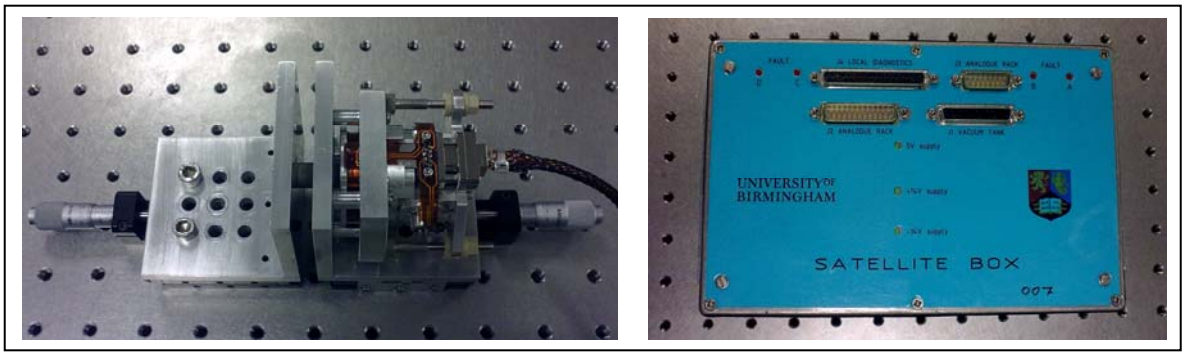

Figure 1. BOSEM Mounted on Test Fixtures and Satellite Box.

2.2 Test Procedure

Measurements of BOSEM noise performance are made at the center of the operating range of the sensor. The first task is therefore to establish the operating range. A DVM can be used to observe the differential output voltage from the Satellite Box amplifier for various positions of the flag as it is translated along the sensing axis of the BOSEM. Figure 2 shows a typical example of the measurement of the BOSEM responsivity. Ideally the differential output voltage should reside between 0 and 20 Volts.

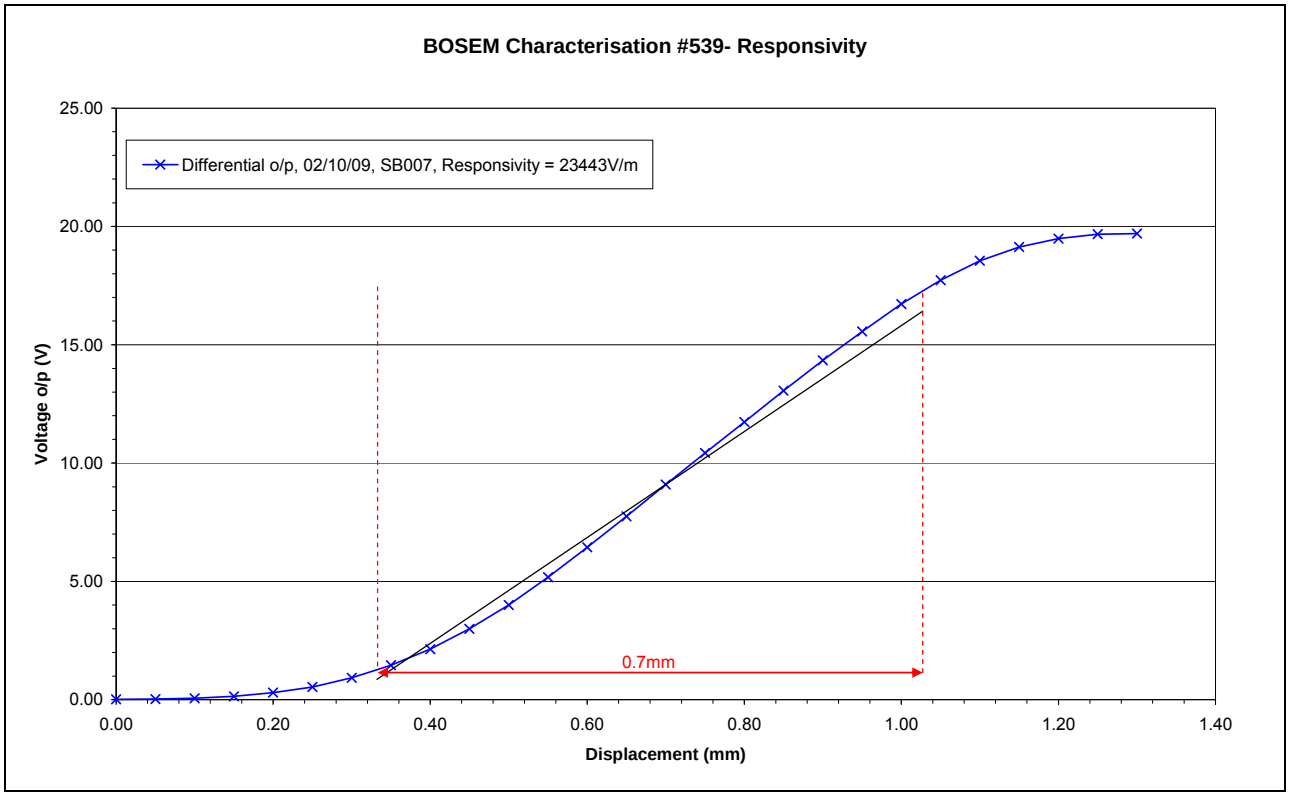

Figure 2. Typical Measured BOSEM Responsivity.

Once the minimum (closed-light) and maximum (open-light) voltages have been indentified the center of operating range can be determined and a noise spectrum taken. Thirty spectra are taken and averaged over the range 0-12.5Hz. Responsivity measurements are repeated any time there's a change in the flag alignment or OSEM configuration.

Note that the requirement [2] placed upon sensor performance is given for the following frequency bands:-

- Worst Case Noise (1-10Hz) $= 3\times10^{-10}$ m/√Hz
- Worst Case Noise (10-20Hz) $= 1\times10^{-10}$ m/√Hz

The sensor is designed to have a ~0.7mm operational range.

During BOSEM production our ATE observed a wider range of PD currents than anticipated, given that we had already screened IRLED output intensities. We therefore selected ten BOSEMs for our sample that lay across the distribution of measured PD currents. Also included were two extreme outliers. A list of BOSEMs under test and their PD current as measured on the ATE is provided in Table 2.

BOSEM Serial #	PD Current (μA)
445	67
474	71
495	65
513	62
527	64
539	69
562	63
575	60
620	56
636	58

Table 2. BOSEMs Under Test.

2.3 Test Results

The results obtained can be seen plotted in Figure 3. The black line represents the requirement and each BOSEM is shown as a different colour trace. The PD currents as measured by the ATE and the measured responsivities are also included within the legend.

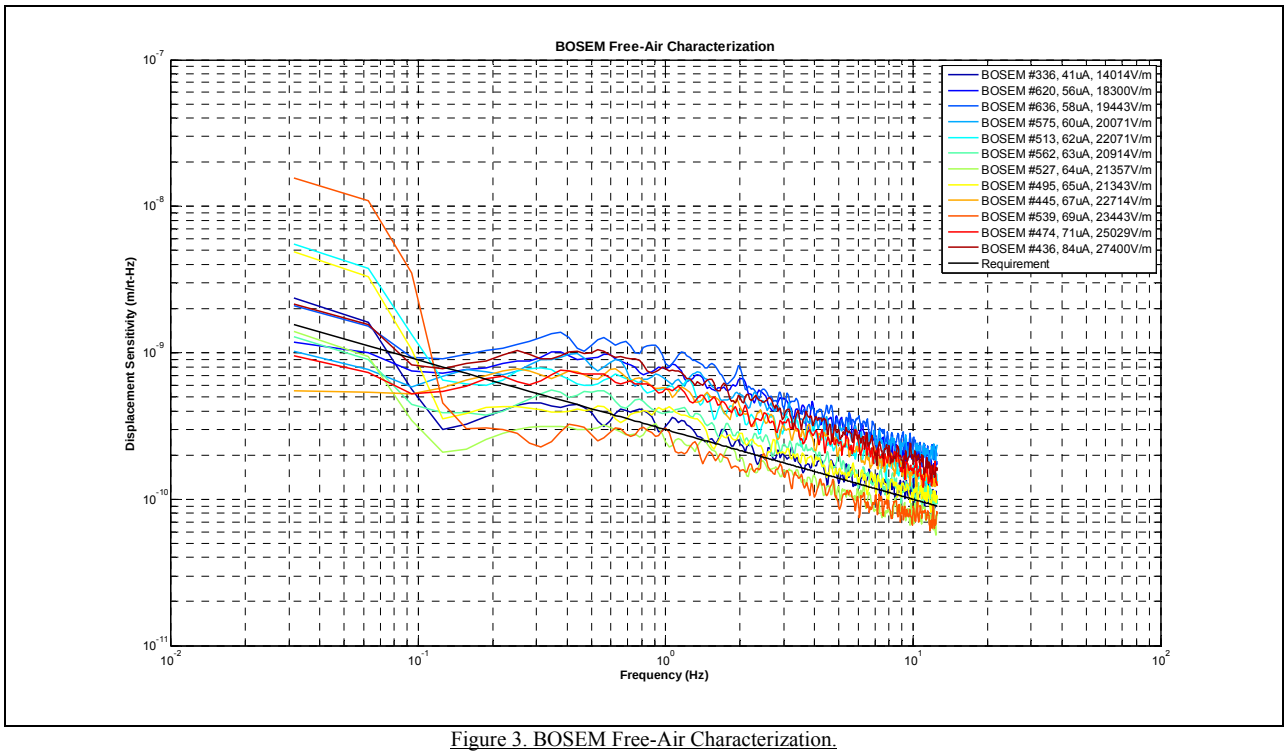

Figure 3. BOSEM Free-Air Characterization.

2.4 Discussion

The distribution of results obtained here is somewhat disappointing, given that in our previous measurements they had met the requirement. It can be seen that for the twelve BOSEMs characterized, two meet the requirement, while the remaining units fail. However we must consider that there are a large number of additional processes that the production units have undergone when compared to bench-top prototype units we tested in the past.

It is therefore vital to determine if any part of the cleaning or bake-out process could have contributed to the observed degradation in noise performance. The use of cleaning solvents, ultra-sonic baths and high temperature bake-outs may have provided ample mechanisms for damage or degradation to occur.

There is no obvious correlation between measured PD current or the responsivity versus BOSEM noise performance. To enable us to identify if the cleaning and baking could have been the cause of the excess noise, the next step is to measure the noise performance of BOSEMs that have not gone through all these additional cleaning and baking processes. For this purpose I reconstituted five old NPOSEMs that were previously employed as screening jigs.

3 NPOSEM Noise Measurements

There have been some very minor developments in the BOSEM design between NPOSEMs and BOSEMs, such as a change of materials (PFA 440 HP to PEEK), but none of these will influence the sensor performance. For a full list of changes please refer to the "Noise Prototype OSEM Design Change Log" [4].

Given these units are not (and never have been) UHV-clean we were able to relax the UHV-clean handing precautions and work with them in a lab-clean environment.

3.1 Test Set-up

The test set-up was exactly the same as described for the BOSEMs in section 2.1.

3.2 Test Procedure

The test procedure was exactly the same as described for the BOSEMs in section 2.2. However we only have five NPOSEMs available and the units tested are listed in Table 3.

NPOSEM Serial #	PD Current (μA)
015	73
032	72
033	71
034	67
035	65

Table 3. NPOSEMs Under Test.

3.3 Test Results

The results obtained can be seen plotted in Figure 4. The black line represents the requirement and each NPOSEM is shown as a different colour trace. The PD currents as measured by the ATE and the measured responsivities are also included within the legend.

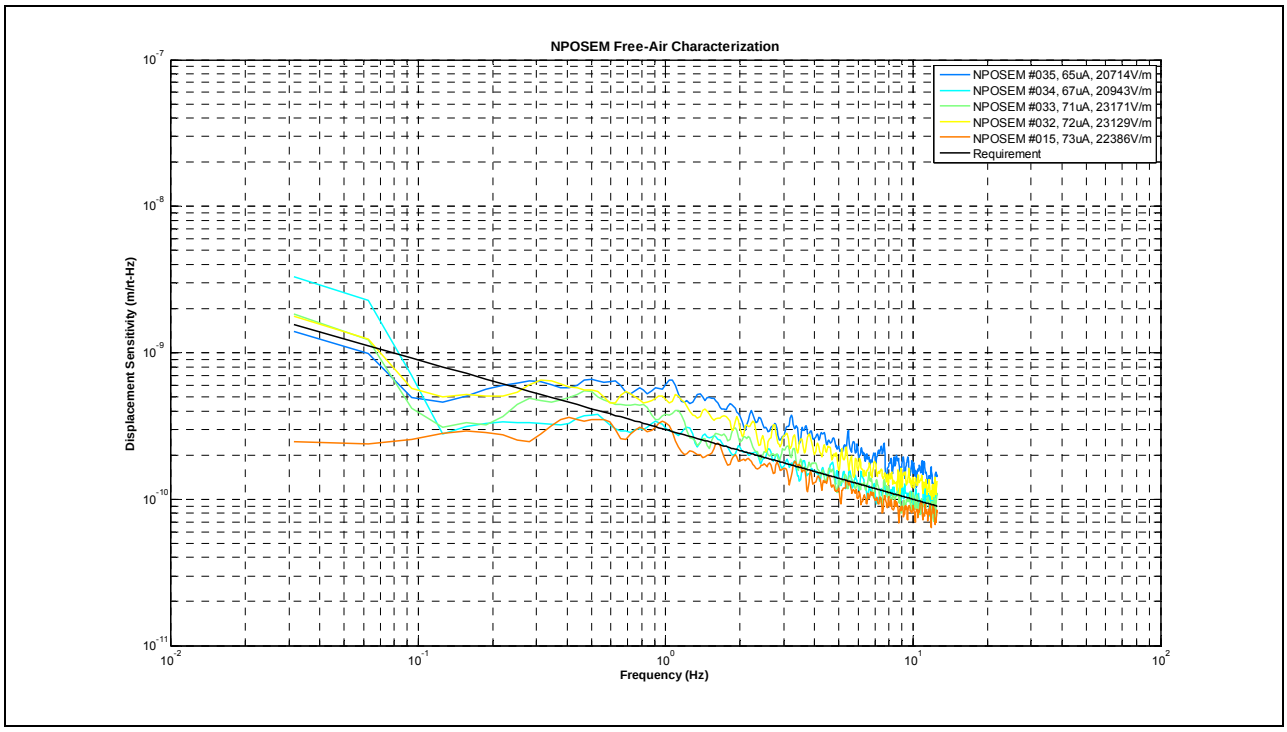

Figure 4. NPOSEM Free-Air Characterization.

3.4 Discussion

It can be seen from Figure 4 that two of the five NPOSEMs characterized appear to meet the requirement. Figure 4 indicates that the distribution of NPOSEM noise performances is very similar to that which was obtained or the BOSEMs in Figure 3. This provides convincing evidence that the noise is inherent within the NPOSEM and has not likely due to any of the additional cleaning and baking processes endured by the BOSEM. Again there is no obvious correlation between measured PD current or the responsivity vs. noise performance.

4 Study into the Source of Excess Noise

As a consequence of the NPOSEM characterization, we now have available two non UHV-clean units, one that meets the requirement (#015) and one that does not (#035). Further tests will aim to establish exactly what the difference is between these two units. A number of target areas have already been identified that necessitate further investigation:-

- Reproducibility
- Flexi-circuit (D050435)
- PD Assembly (D060217)
- IRLED Assembly (D060216)

Each of these areas is addressed in subsequent sections of this report. To help familiarize the reader with the configuration of key functional components of the BOSEM Figure 5 provides a simplified view. Figure 6 provides a cross-section through IRLED carrier assembly and a part explosion of each component. Figure 7 shows the equivalent cross-section and part explosion for the PD carrier.

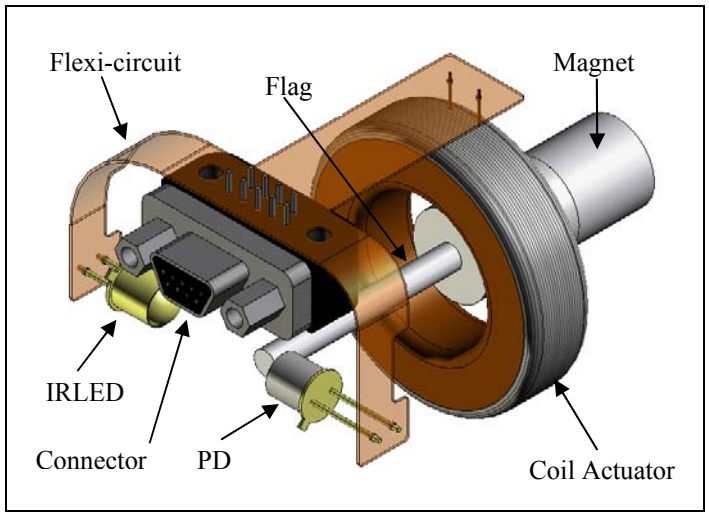

Figure 5. Configuration of BOSEM Key Functional Components

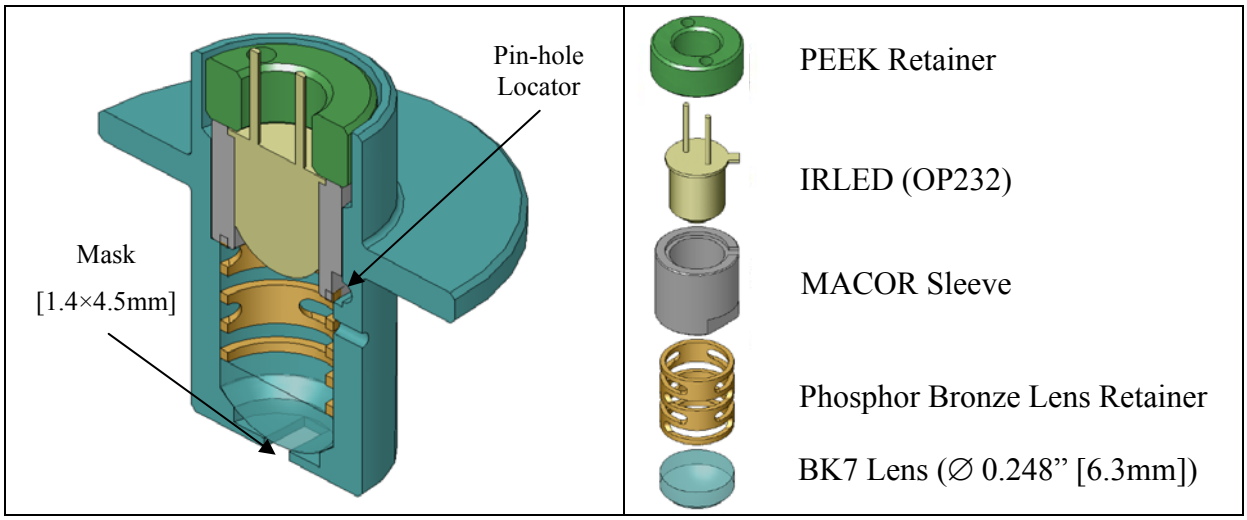

Figure 6. IRLED Carrier Section and Part Explosion

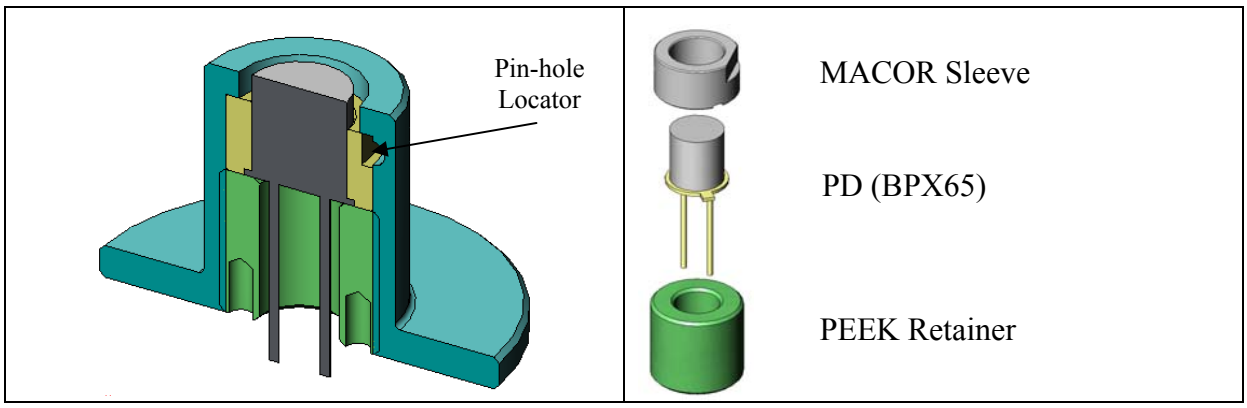

Figure 7. PD Carrier Section and Part Explosion

4.1 Reproducibility

It is crucial to demonstrate reproducibility in our noise performance measurements. For subsequent tests it will be necessary to disassemble the NPOSEM to varying extents. We need to be confident that if we were to disassemble and then reassemble the unit again, it would exhibit repeatable noise performance on each occasion. Otherwise it's possible that mechanical tolerances or slight deviations from the assembly procedure [3] could conspire to give inconsistent results and would make studying the source of excess noise much more challenging.

4.1.1 Test Set-up

The test set-up was consistent with that described for the BOSEMs in section 2.1.

4.1.2 Test Procedure

The test procedure was exactly the same as described for the BOSEMs in section 2.2. However, on this occasion two NPOSEMs were used for this test. A unit was selected that has been observed to meet the requirement (NPOSEM #015). Also a unit that exhibited the largest excess noise was also selected (NPOSEM #035).

Prior to commencing the noise measurement, each units sensor carriers were completely disassembled, then reassembled, before being integrated onto the test fixtures again.

4.1.3 Test Results

The results obtained can be seen plotted in Figure 8. The black line represents the requirement and the "original build" and "reassembled" NPOSEM results are shown in a different colour traces.

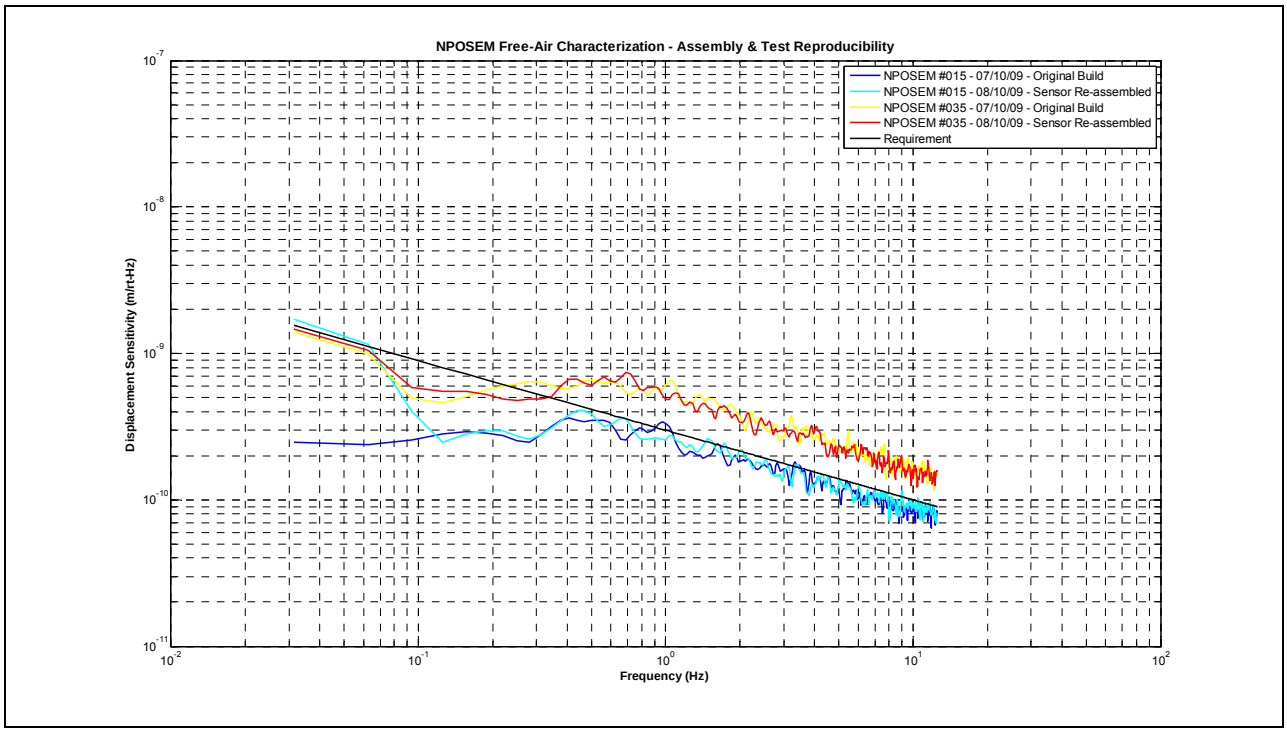

Figure 8. Assembly and Test Reproducibility.

4.1.4 Discussion

The results shown is Figure 8 demonstrate that in each case there is a great deal of reproducibility in both in the experimental technique and in the assembly of the sensor. This is very encouraging for further tests that will be conducted.

4.2 Flexi-circuit Investigation

The flexi-circuit is one area where we have encountered problems in the past. Manufacturing issues have been evident that have led to partial and complete failure of this part. However, after a number of iterations of the design and detailed discussions with the manufacturer we believe we have been successful in overcoming these issues for the production run.

To verify the correct operation of the flexi-circuit, a straightforward test can be carried out. Each arm of the flexi-circuit that reaches to either the PD or IRLED can simply be bypassed with jump-wires. If there were sub-surface defects within the flex-circuit structure that could be exacerbated by bending the flexible arms or by soldering to the PD or IRLED, then these issues would be clearly distinguishable.

4.2.1 Test Set-up

The test set-up was consistent with that described for the BOSEMs in section 2.1.

4.2.2 Test Procedure

The test procedure was the same as described for the BOSEMs in section 2.2. However, on this occasion only a single NPOSEM was selected. The unit selected was one that had exhibited the largest excess noise (NPOSEM #035).

Prior to commencing the test a few modifications had to be made, with noise measurements being taken at each stage:-

1) The PD arm of the flexi-circuit was bypassed with jump-wires.
2) The IRLED arm of the flexi-circuit was bypassed with jump-wires.
3) All connections on the flexi-circuit were de-fluxed with a cleaning solvent.

It was not necessary to measure the responsivity again in each of the above cases, given that the NPOSEM under test was left on the test fixtures while the modifications were made to the flexi-circuit in-situ.

4.2.3 Test Results

The results obtained can be seen plotted in Figure 9. The black line represents the requirement and each colour traces represents the modification made to the flexi-circuit denoted in the legend.

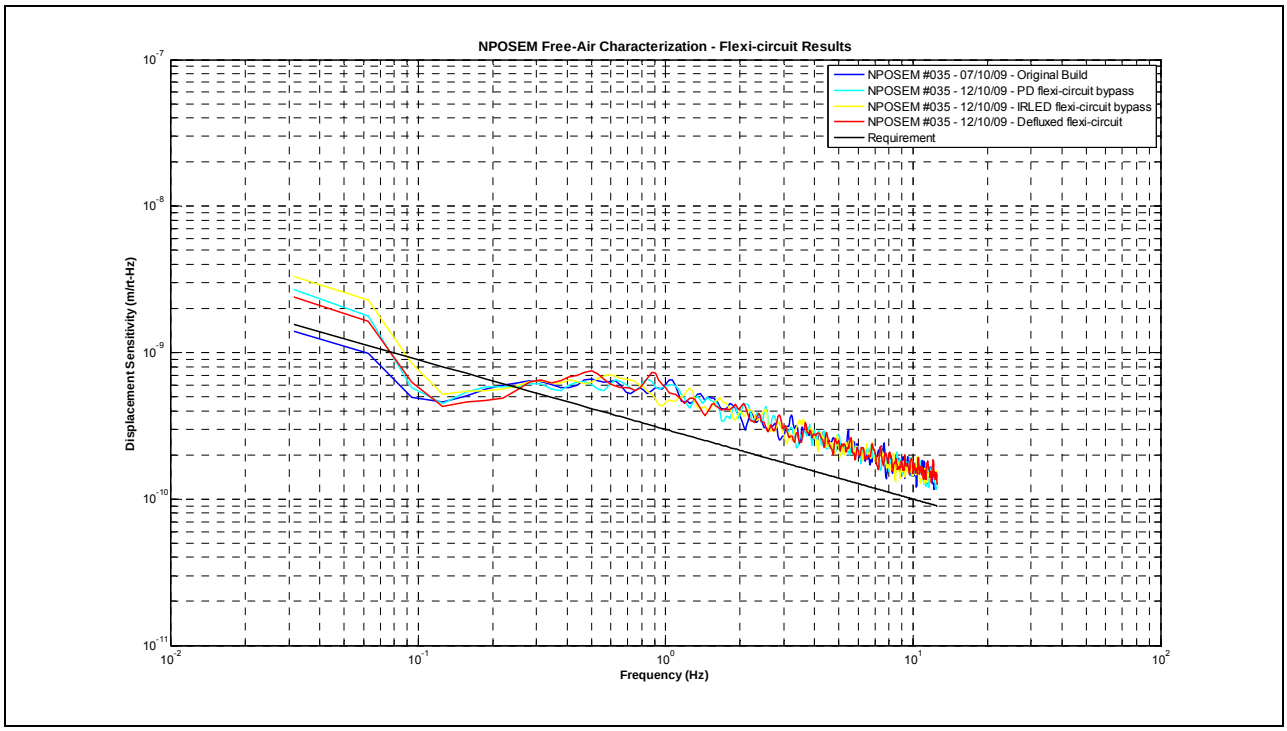

Figure 9. NPOSEM #035 Flexi-circuit Results.

4.2.4 Discussion

It is clear to see from the results plotted in Figure 9 that there is no improvement in noise performance by bypassing the flexi-circuit. Therefore the flex-circuit is not the cause the excess noise.

4.3 Sensor Investigation

There are two key components of the sensor assembly, the PD and IRLED. At this stage we now need to be able to eliminate either the PD or the IRLED from our investigation. This can be achieved by exchanging working and miss-behaving PDs and IRLEDs between NPOSEMs. In addition, complete carrier assemblies and individual PD / IRLED devices can be exchanged to establish if the issue resides within the device itself or with its associated carrier assembly.

4.3.1 Test Set-up

The test set-up was consistent with that described for the BOSEMs in section 2.1.

4.3.2 Test Procedure

The test procedure was exactly the same as described for the BOSEMs in section 2.2. However, on this occasion two NPOSEMs were selected. A unit was selected that has been observed to meet the requirement (NPOSEM #015). Also a unit that exhibited the largest excess noise was also selected (NPOSEM #035).

Prior to commencing the test some modifications had to be made to NPOSEM #015, with noise measurements being taken at each stage:-

1) The complete PD carrier assembly from NPOSEM #035 is switched into NPOSEM #015.
2) Just the PD device from NPOSEM #035 is switched into NPOSEM #015.

For verification the same process was carried out on NPOSEM #035, with noise measurements being taken at each stage:-

3) The complete PD carrier assembly from NPOSEM #015 is switched into NPOSEM #035.
4) Just the PD device from NPOSEM #015 is switched into NPOSEM #035.

4.3.3 Test Results

The noise measurements obtained for NPOSEM #015 from test steps (1) and (2) can be seen plotted in Figure 10. Noise measurements obtained for NPOSEM #035 from test steps (3) and (4) can be seen plotted in Figure 11. Again the black line represents the requirement and the colour traces denote each configuration (1) through (4) detailed above.

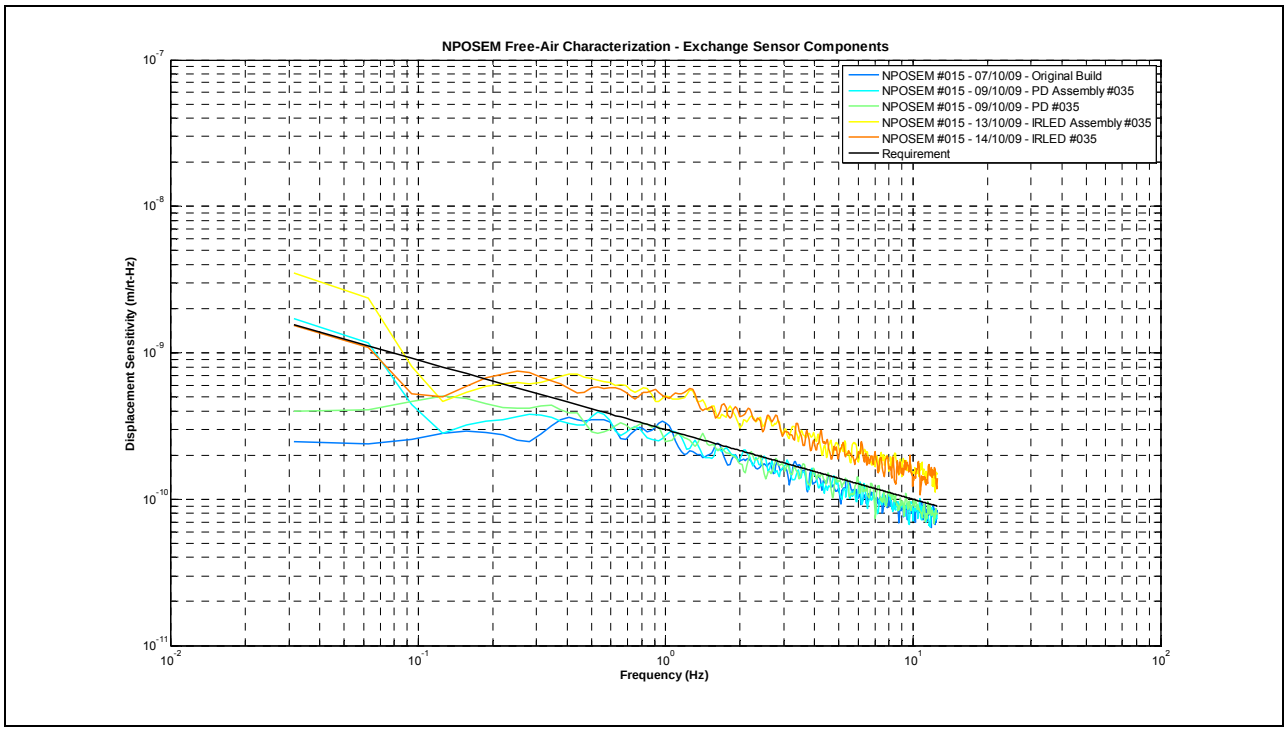

Figure 10. Exchange of Sensor Components for NPOSEM #015.

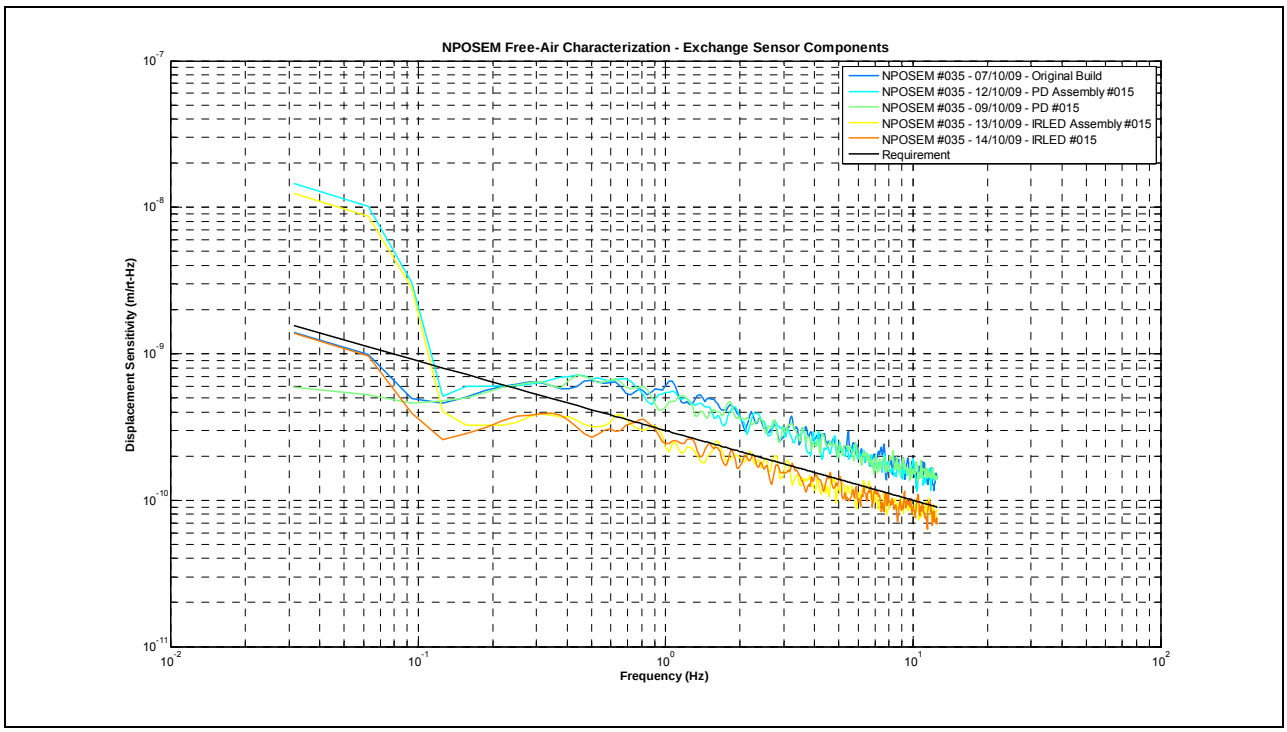

Figure 11. Exchange of Sensor Components for NPOSEM #035.

4.3.4 Discussion

The noise plots obtained show that exchanging the PD between NPOSEMs #015 and #035 makes no difference to the sensitivity performance obtained. However exchanging the IRLED devices has a significant impact upon the performance. This provides strong evidence that the IRLED itself is the cause of the excess noise. However, it is still necessary to establish if it is a geometric feature of the IRLEDs assembly or noise that is intrinsic to the device that is the source of the excess noise.

4.4 Open-light Investigation

It is desirable to speed-up the BOSEM characterization procedure. The measurements taken up until now are quite involved and not ideally suited for enabling the quick characterization of a BOSEM. By removing the translatable flag it will no longer be possible to make any responsivity measurements, which shall significantly simplify the measurement procedure. Instead noise measurements will be made in an "open-light" configuration. This should also help shed light into finding out if the source of excess noise is due to the IRLED or the geometry of the NPOSEM.

4.4.1 Test Set-up

The test set-up is consistent with that described for the BOSEMs in section 2.1. However the flag is withdrawn completely from the NPOSEM. Two configurations of test set-up have been used for the open-light photo-current characterization:-

1) Open-light measurement, IRLED and PD mounted within BOSEM.
2) Open-light measurement, IRLED and PD mounted using external fixture (see section 5.1).

4.4.2 Test Procedure

Open-light photo-current noise measurements are conducted for all NPOSEMS. Note that it was not necessary to measure the responsivity for any of the units.

4.4.3 Test Results

Open-light photo-current noise measurements obtained for all NPOSEMs can be seen plotted in Figure 12. Open-light measurements for the IRLED and PD mounted in an external fixture can be seen in Figure 13.

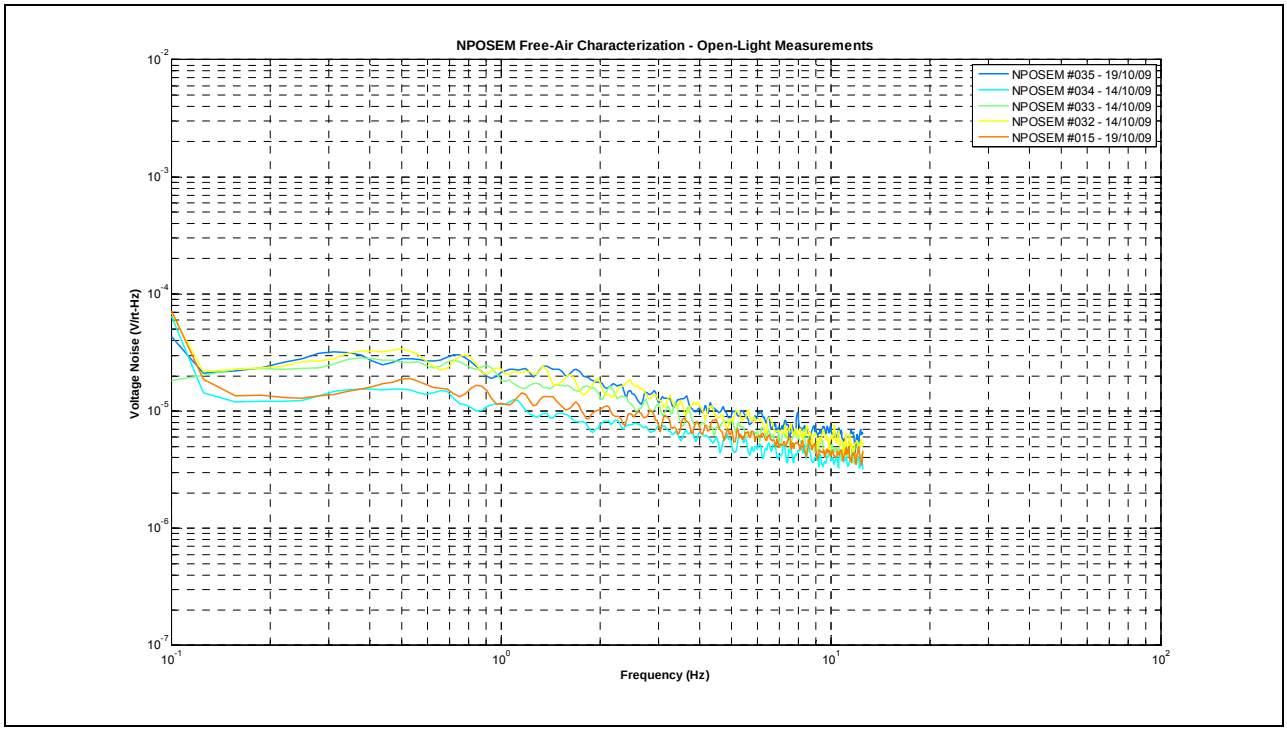

Figure 12. IRLED and PD Open-light Measurements (mounted within NPOSEM).

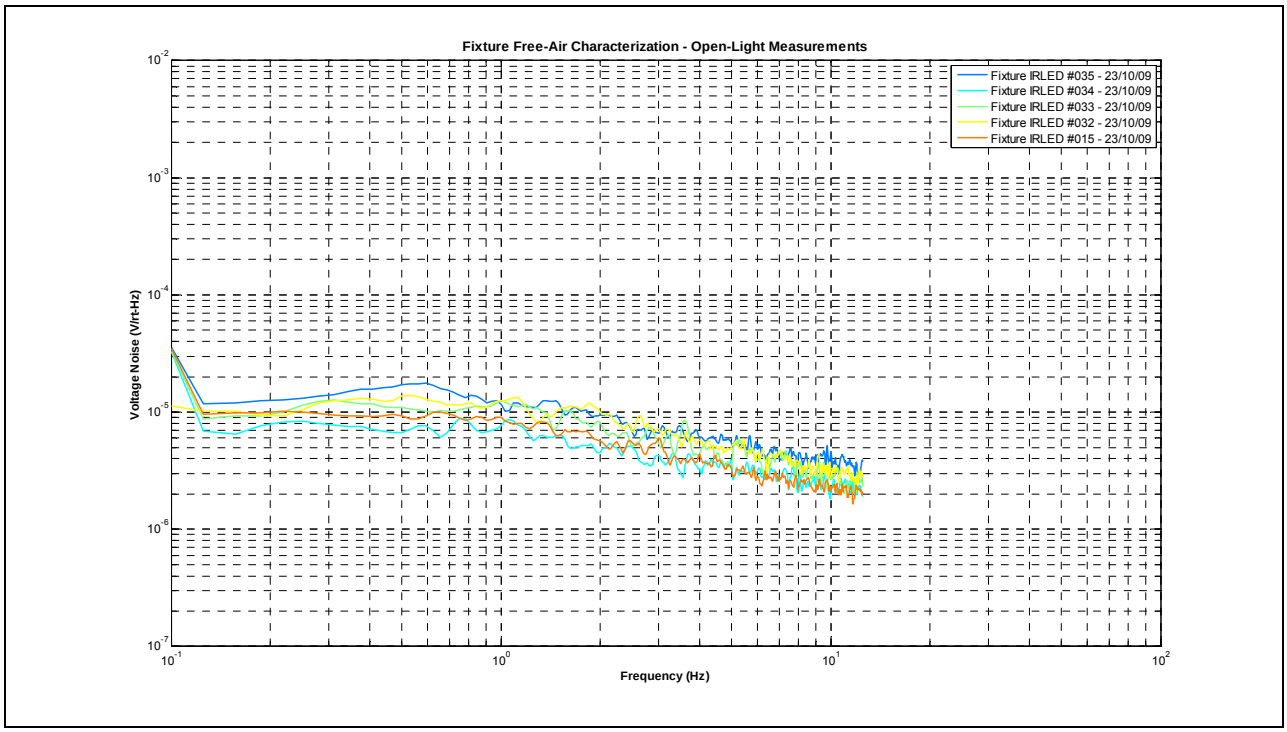

Figure 13. IRLED and PD Open-light Measurements (mounted within external fixtures).

4.4.4 Discussion

The IRLEDs and PDs can be observed to exhibit a very consistent photo-current noise relative to each other. This occurs both when mounted within the NPOSEM and when mounted using the external fixture. This suggests that the noise is independent of the geometry of the NPOSEM, or the positioning of the lens in the IRLED carrier assembly.

4.5 Axial Symmetry Investigation

The axial orientation of the IRELD and PD are constrained when the devices are installed into the BOSEM. This is necessary to ensure the correct lead polarity, when connecting to the flexi-circuit. The orientation is maintained by means of a pin-hole locater, which when a pin is inserted, locks them in place during the assembly process. This can be seen on Figure 6 for the IRLED and Figure 7 for the PD.

It is conceivable that there could be minor misalignments (<5°) in the final orientation of the device. It is therefore worthwhile ensuring that the excess noise is not sensitive to the rotation of the IRLED about its emission axis.

4.5.1 Test Set-up

The test set-up is consistent with that described for the IRLED and PD in section 4.4.1. The open-light configuration using the test fixtures is used. The IRLED mount has the capability to rotate the device through 360°.

4.5.2 Test Procedure

Open-light noise measurements are conducted for a single IRLED #032. Noise measurements are made with the IRLED at each of the following orientations:-

1) Nominal (the standard orientation wrt the PD when installed into the BOSEM)
2) + 10°
3) + 20°
4) + 90°
5) + 180°
6) + 270°

Note that it was not necessary to measure the responsivity.

4.5.3 Test Results

The noise measurements obtained for IRLED #032 for orientation (1) through to (6) can be seen plotted in Figure 14.

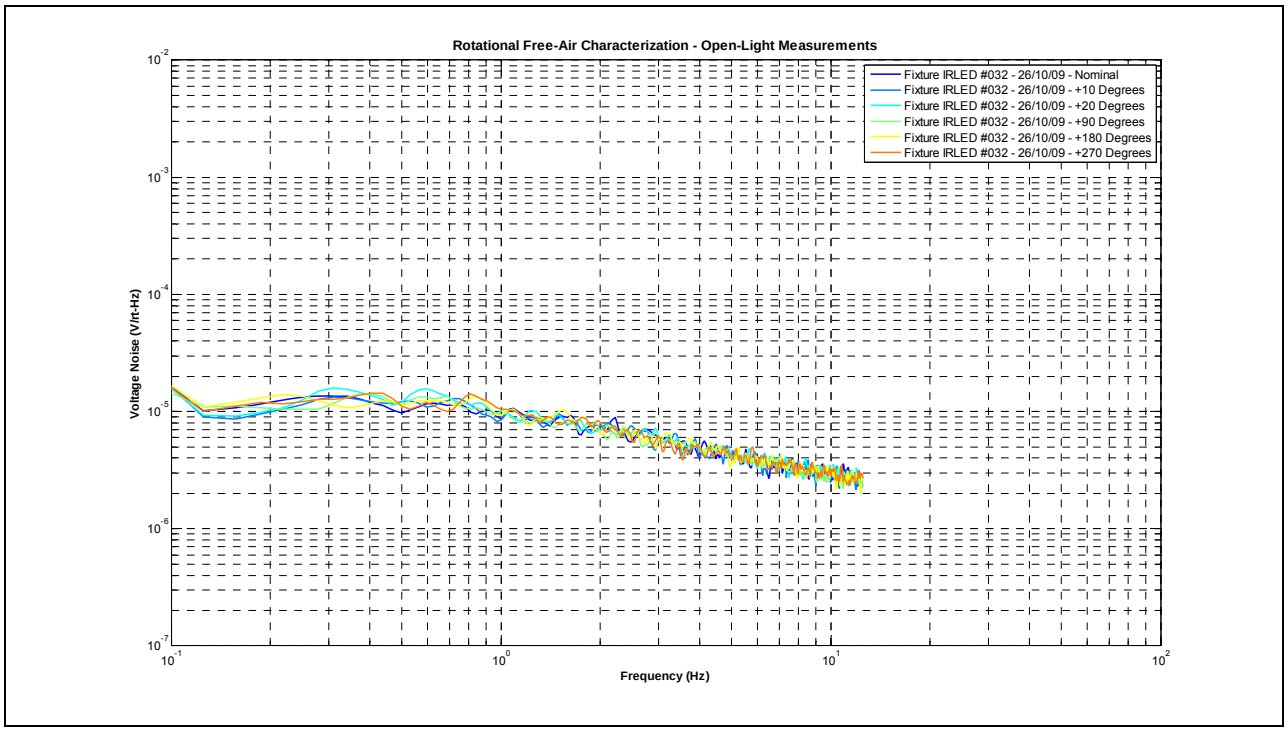

Figure 14. IRLED and PD Open-light Measurements (mounted within external fixtures).

4.5.4 Discussion

These results shown in Figure 14 indicate that photo-current noise emissions from the IRLED are axially symmetric i.e. there is no dependence on the final orientation of the device.

4.6 Thermal Environment

When assembled into a BOSEM the IRLED is located within a MACOR sleeve (see Figure 6). This is to provide electrical isolation of the device i.e. to ensure no currents are flowing through the suspension structure. It is conceivable that the low frequency noise of the device is affected by the thermal environment of the IRLED. All bench-top prototyping work conducted by ourselves and our collaborator, Nick Lockerbie at the University of Strathclyde, was conduced using metallic sleeves with high thermal conductivity (6061/6082 Aluminum, 170 W/m-K). Therefore the final BOSEM design may not represent the optimal thermal environment for the IRLED. In these tests we aim to measure the BOSEM performance for different thermal conductivities of IRLED sleeve.

4.6.1 Test Set-up

The test set-up was exactly the same as described for the BOSEM in section 2.1.

4.6.2 Test Procedure

The test procedure was exactly the same as described for the BOSEMs in section 2.2. However we only require one NPOSEM (#015) for these tests. The test procedure is repeated for the following different configurations of the IRLED carrier assembly:-

1) As built configuration (MACOR sleeve).
2) Alumina Sleeve.
3) Alumina Sleeve and Thermal Paste at all critical interfaces.

4.6.3 Test Results

The noise measurements obtained for NPOSEM #015 for configurations (1) through to (3) can be seen plotted in Figure 15.

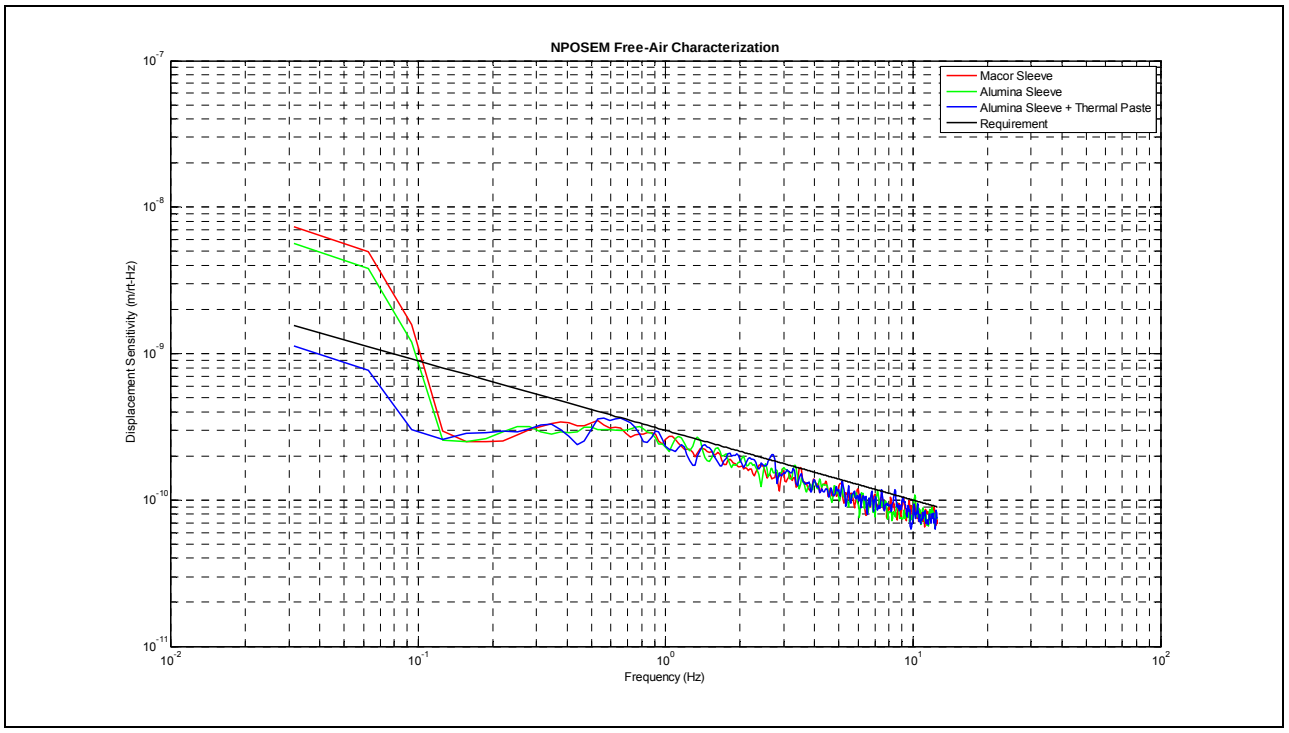

Figure 15. IRLED Thermal Environment (conductivity) Study Results.

4.6.4 Discussion

The results plotted in Figure 15 show no discernable improvement in noise performance by increasing the thermal conductivity of the MACOR sleeve (1.46 W/m-K) to Alumina sleeve (26 W/m-K). Therefore there would apparently be nothing to gain by switching to Alumina for the IRLED sleeve material.

4.7 Lens Geometry Investigation

There are two lenses used by the BOSEM IRLED carrier assembly. Within the actual IRLED package is an integrated lens, in addition we use a separate ∅6.3mm plano-convex lens to improve the collimation of the beam.

During a much earlier phase of the project, both we and a collaborator at the University of Strathclyde (Nick Lockerbie) were involved in a "sensor study" to determine the optical configuration. This involved identifying the best candidate IRLED / PD and optimizing the optical layout. It could be possible that the lens geometry of the production batch IRLEDs differs from that found during the sensor study. Ideally we would wish to control the separation between the IRLED device and the plano-convex collimating lens. However, this is not easily to accommodate within the final production BOSEM, so alternatively we can investigate the noise performance for a range of lenses of varying focal length.

4.7.1 Test Set-up

The test set-up is consistent with that described for the BOSEMs in section 2.1. In addition the following lenses are to be used to replace the standard "as built" configuration:-

1) ∅6.3mm lens with FL = 8mm (standard as built configuration)
2) ∅6.3mm lens with FL = 8mm (Anti-Reflection coated)
3) ∅6.3mm lens with FL = 10mm
4) ∅6.3mm lens with FL = 12mm
5) ∅6.3mm lens with FL = 16mm
6) ∅6.3mm lens with FL = 20mm
7) ∅6.3mm lens removed

4.7.2 Test Procedure

The test procedure was exactly the same as described for the BOSEMs in section 2.2. However, the only NPOSEM under test was unit #035.

4.7.3 Test Results

The noise measurements obtained for NPOSEM #035 for configurations (1) through to (7) can be seen plotted in Figure 16.

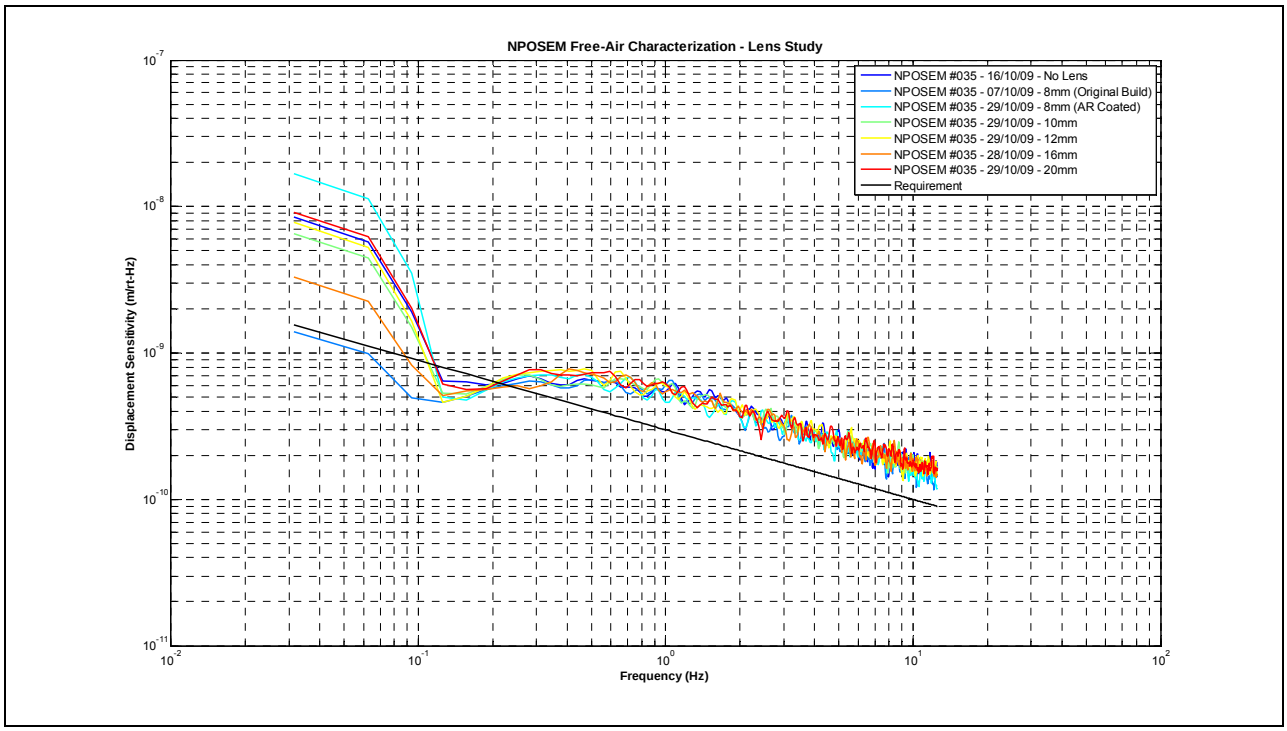

Figure 16. Lens Optimization Study Results.

4.7.4 Discussion

For the unit under test it can be observed that changing the focal length of the additional collimation lens has no discernable effect upon the noise performance of the NPOSEM. Also the presence of the anti-reflection coating on the lens has negligible impact upon performance. These results add weight to the argument that the geometry of the sensor is not the most important factor in determining its noise performance. For this reason subsequent tests will concentrate upon the properties of the IRLED itself.

5 IRLED Screening

It is now necessary to investigate the properties of the IRLED more comprehensively. The aim is to fully characterize a sample quantity of IRLEDs. Capturing these results will enable us to more easily observe correlations between any of the parameters measured and the final noise performance of a BOSEM. This will allow us to determine what properties of the IRLED are desirable for ensuring that the BOSEM noise performance meets the requirement. There are a number of IRLED parameters that can be readily measured for each device:-

1) Forward voltage
2) Distance to the focal plane
3) Open-light photo-current noise

To give us confidence that we are screening the correct parameters it will be necessary to verify that our screened IRLEDs enable a NPOSEM to meet the performance requirements, where it had not done so before in its original 'as built' configuration.

5.1 Test Set-up

The test set-up is consistent with that described for the BOSEMs in section 2.1. However we use a simple external fixture to mount the IRLED and PD as can be seen in Figure 17. The devices are held within PTFE inserts and can be translated along the emission axis of the IRLED. Concentricity of the IRLED and PD is maintained throughout.

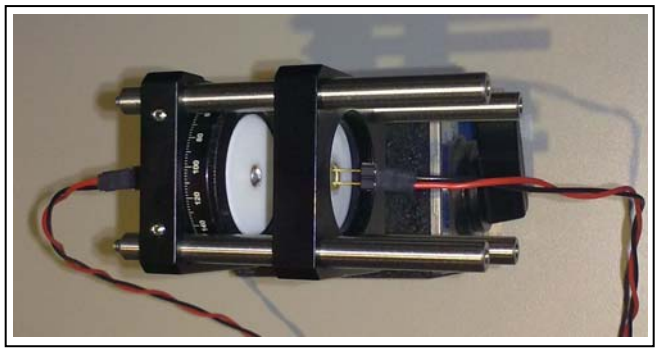

Figure 17. External Open-light Fixture.

5.2 Test Procedure

Each IRLED is push fit into the PTFE insert enabling multiple devices to be swapped in and out relatively quickly. Note that the same PD device is used throughout the duration of these tests. Under normal operating conditions (i.e. 35mA drive current) we can measure and record the forward voltage across the IRLED. Next the PD can be translated along the fixture until the focal

plane of the IRLED is reached. At this location the PD stage can be locked in place and the distance between it and the IRLED noted. The set-up is then shielded from any ambient or stray light by means of opaque enclosure placed over the top.

5.3 Production Batch IRLEDs

We have already characterized the open-light performance of IRLEDs from the five NPOSEMs using an external fixture, as can be seen in Figure 13 (section 4.43). To compliment these results the forward voltage and focal planes have also been measured for these devices.

The production batch of IRLEDs was procured a number of years ago. All of these devices have since gone through a burn-in process as described in the BOSEM design document [2]. This prescribed that the devices be burned-in at their maximum rated forward current of 100mA for 50 hours duration. All of these devices were then consequently screened for output intensity, with some of the extreme cases being rejected. Five of the rejected IRLEDs (#??1 to #??5) have gone through additional screening as well as five devices that were not rejected (#??6 to #?10).

The results captured show a spread in the forward voltage of the devices of 110mV and a focal plane spread of 2.64mm. Figure 18 shows a plot of open-light photo-current noise measurements for the production batch IRLEDs discussed above. In addition the trace shown in black is included to represent NPOSEM #034 (i.e. a unit that just met the requirement).

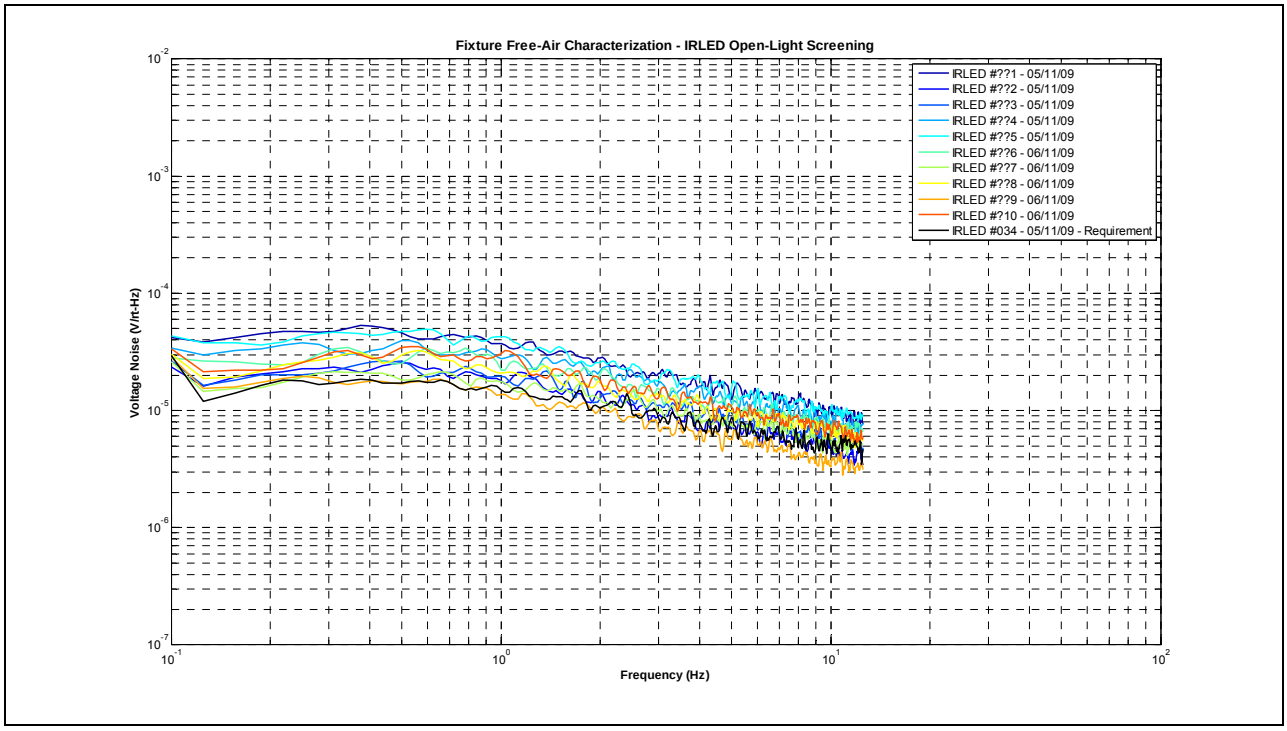

Figure 18. Production Batch IRLED Open-light Photo-current Noise Results.

It is now important to verify that an IRLED device that demonstrates comparatively low open-light photo-current noise is still capable of meeting the requirement when installed into a NPOSEM.

5.4 Verification of IRLED Screening

An IRLED device indentified during the screening process (#??9), whose open-light photo-current noise appears to meet the requirement is installed into NPOSEM #035. As built, NPOSEM #035 did not meet the requirement. Figure 19 shows the noise measurements for this NPOSEM before (in red) and after (in green) the screened IRLED was fitted. Note that the MACOR sleeve and collimation lens were known to be damaged in this unit. These were replaced and the measurement repeated (in blue).

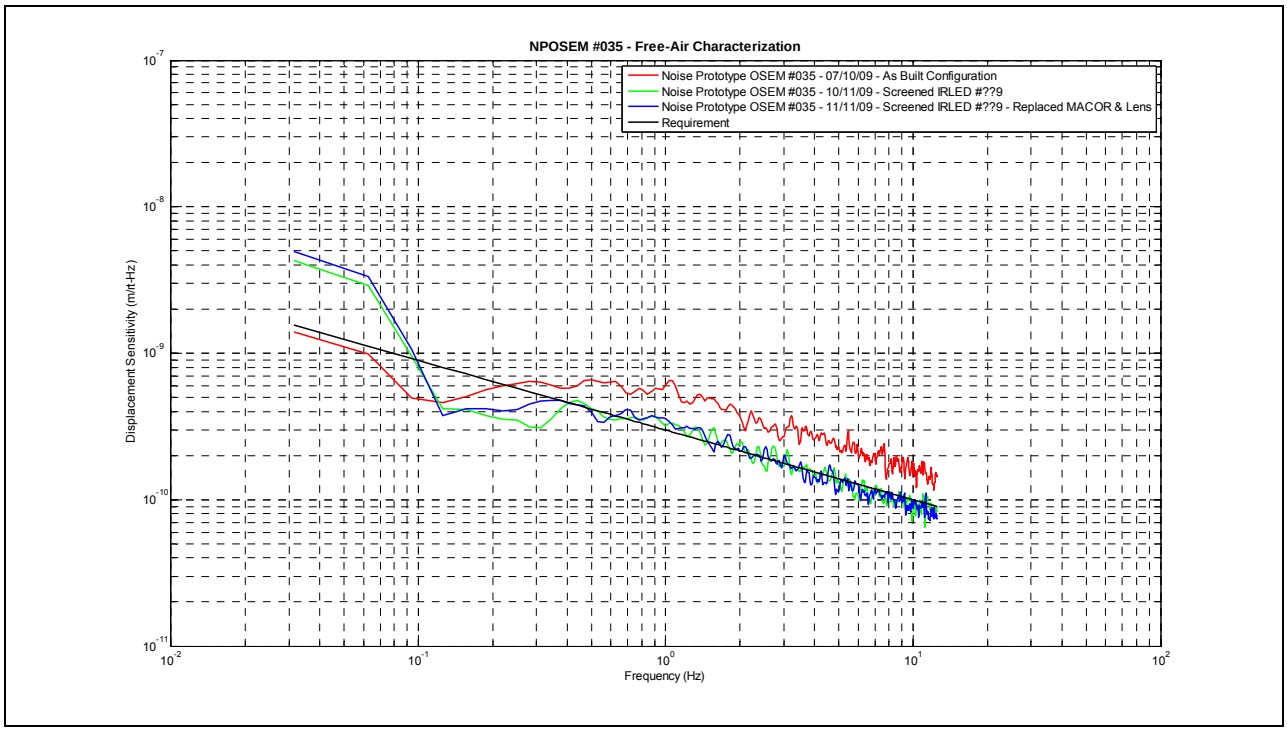

Figure 19. Characterization of NPOSEM #035 before and after installation of screened IRLED.

It can be observed from Figure 19, that replacing the IRLED with a noise screened IRLED improved the noise performance of the NPOSEM, so that it coincided with the performance requirement.

It has been suggested in some of the literature [5] that accelerated life tests i.e. by burning-in the IRLED could potentially cause an increase in the 1/f voltage noise of the device. So it was thought that obtaining a new batch of commercial off-the-shelf (COTS) IRLEDs would be useful to investigate if our burn-in tests had inadvertently degraded their 1/f noise performance.

5.5 COTS Batch IRLED Results

An additional 27 devices were procured of exactly the same OP232 devices used in our production batch. However these 27 would not be burned-in and would instead have their off-the-shelf performance characterized immediately.

The characterization results captured show a spread in the forward voltage of the devices of 50mV and a focal plane spread of 2.67mm. Figure 20 shows a plot of open-light photo-current noise measurements for the COTS batch of IRLEDs (#?11 to #?37). Again the trace shown in black is included to represent NPOSEM #034 (i.e. a unit that just met the requirement).

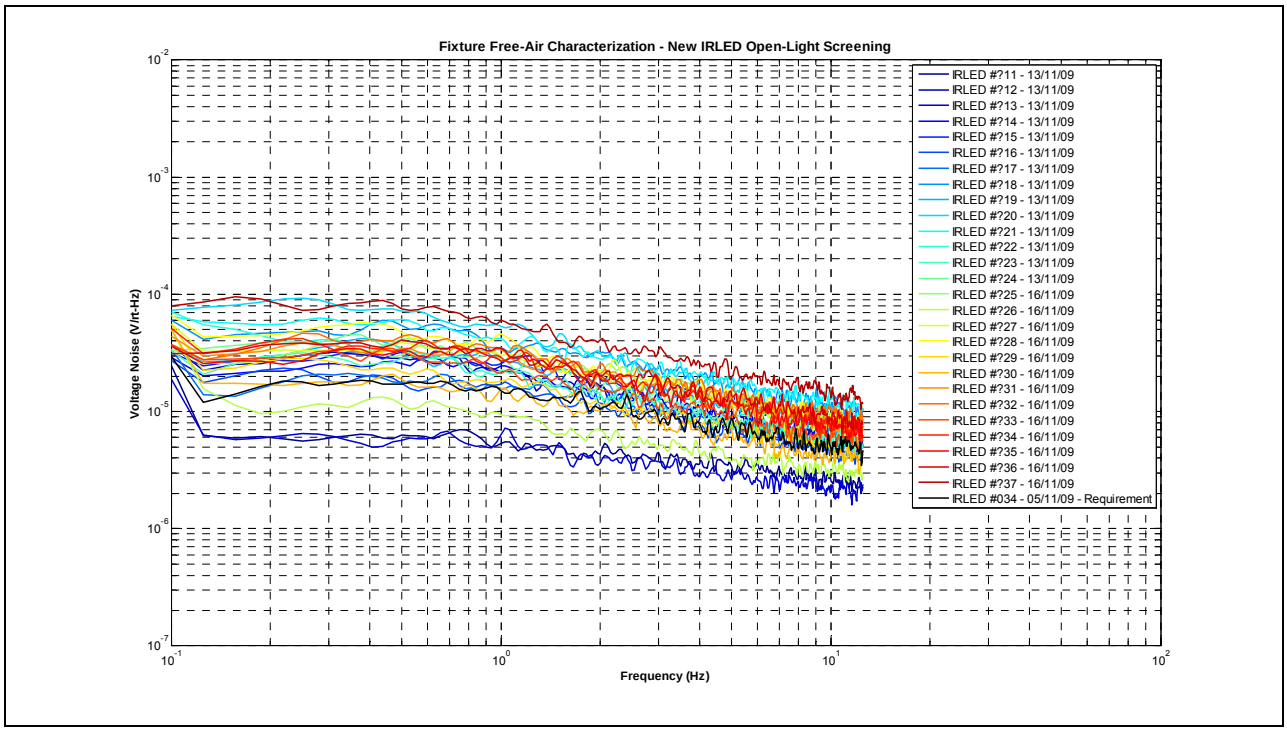

Figure 20. COTS Batch IRLED Open-light Photo-current Noise Results.

From Figure 20 it can be seen that the spread in noise performance is larger for the COTS batch of IRLEDs than it appears for the production batch of IRLEDs. It does not appear that the burn-in of the production IRLEDs has been detrimental to the noise performance (this is investigated more comprehensively in section 5.7).

However, there are a couple of interesting candidates in the COTS batch. IRLEDs #?11 and #?13 are observed to exhibit significantly lower photo-current noise when compared with the rest of the batch. This performance will now be verified by installing these devices into NPOSEMs.

5.6 Verification of IRLED Screening

IRLED #?13, indentified during the screening process, whose open-light photo-current noise appears to meet the requirement, with significant margin, is installed into NPOSEM #032. As built, NPOSEM #032 did not meet the requirement. Figure 21 shows the noise measurements for this NPOSEM before (in red) and after (in green) the screened IRLED was fitted. Note that the responsivity of this NPOSEM increased by approximately 30% indicating that this IRLEDs is particularly efficient.

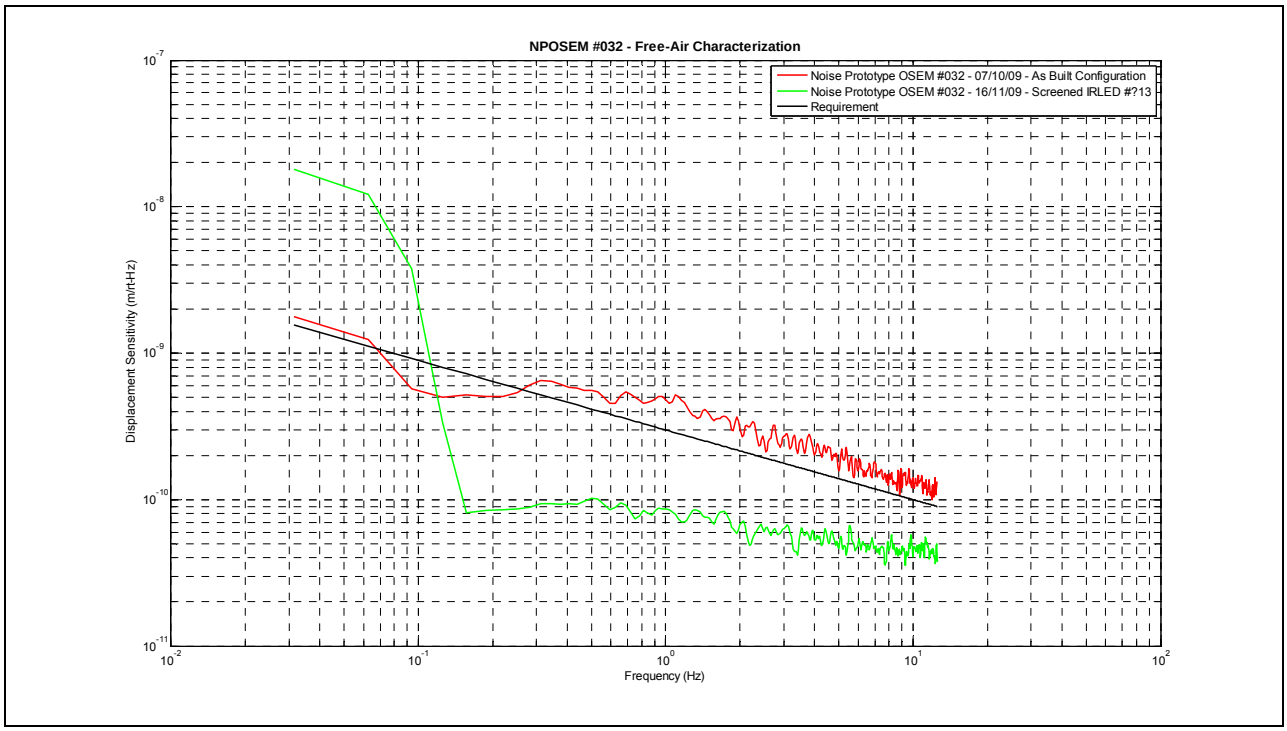

Figure 21. Characterization of NPOSEM #032 before and after installation of screened IRLED.

It can be observed from Figure 21 that replacing the IRLED with a comparatively lower photo-current noise, screened device, significantly improves the NPOSEMs noise performance. These very low noise measurements appear to concur with previous measurements taken by our collaborator, Nick Lockerbie, at the University of Strathclyde [6]. However, it should be noted that a surface mount PD and a slightly different optical configuration was employed in the Strathclyde set-up. Until now, we had been unable to reproduce this level of performance at Birmingham.

It is presently unknown if similar low photo-current noise IRLEDs exist in our production batch. It is possible that the burn-in process could have degraded their performance, or they could have been rejected as part of our intensity screening scheme, since they may have been considered extremely efficient.

5.7 Burn-in Investigation

It can be seen by comparing the photo-current noise in Figure 18 and Figure 20, that there is a wider distribution of results for the COTS IRLEDs than for our production batch. In addition there are also a couple of devices in the COTS batch that exhibit much lower photo-current noise when compared with other IRLEDs. Such low photo-current noise IRLEDs have so far not been observed in our production batch and it is our concern that the burn-in process could have caused degradation of the photo-current noise for in these devices.

The aim of these tests is to establish if the burn-in process has contributed to the excess noise observed in the production BOSEMs. For these tests 4 COSTS IRLEDs were selected; 2 that exhibited the lowest photo-current noise (#?11 & #?13) and 2 that exhibited the highest (#?20 & #?37). Open-light measurements were made of the photo-current noise for a range of different burn-in durations. Initially the units were measured at time zero (i.e. after no burn-in at all) and then after 25 hours and 94 hours duration. The burn-in was carried out at the maximum forward current rating of the IRLED (100mA) and forced air cooling used throughout. A final measurement was made after leaving the devices under burn-in conditions, but with the forced air cooling turned off. With this final configuration we would hope to simulate the "worst-case" burn-in conditions and thermal stress environment for the device.

Figure 22 shows the photo-current noise measurements obtained at each stage of the burn-in process. It can be seen that photo-current noise for each device is apparently unaffected by the burn-in process. Each IRLED device maintains a consistent level of noise performance both before and after burn-in. Even in the "worst-case" scenario, the IRLED devices still maintain a similar photo-current noise performance as they achieved prior to the start of the burn-in process.

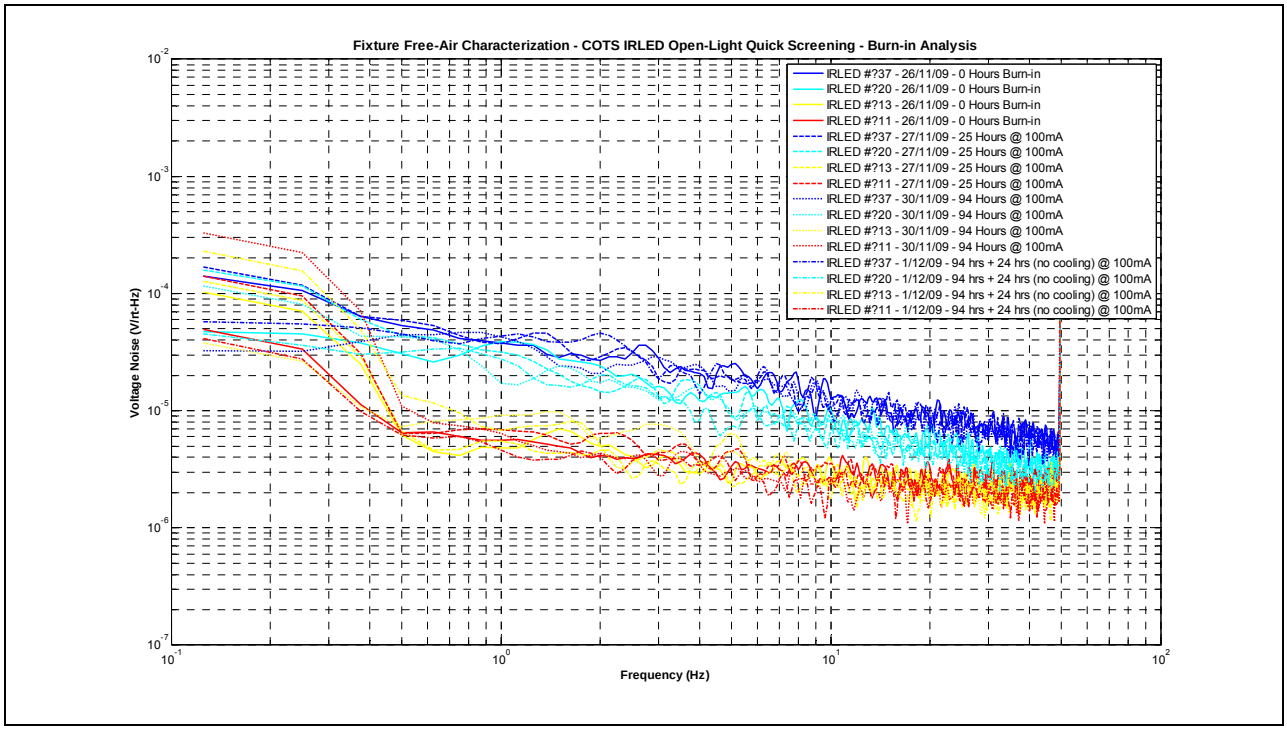

Figure 22. COTS IRLEDs Photo-current Noise for a Range of Burn-in Conditions.

These results are very encouraging as they suggest that nothing we have done to the devices since taking delivery could have degraded noise performance, thus confirming that we are purely looking at device-to-device manufacturing variations in IRLEDs.

5.8 IRLED Package Dissection

The measurements we have taken thus far have demonstrated that the excess noise is intrinsic to the IRLED. However we are still seeking to identify the mechanism which is responsible. The IRLED packages contain an integral lens and I have observed a wide range of focal lengths in the devices characterized. This indicates significant variation in the manufacturer's placement of this internal lens. It's conceivable that this lens may not have an anti-reflection coating on internal surfaces and as a consequence there could be back-reflections de-stabilizing the device. An OP232 device was selected that had demonstrated a large amount of excess noise. A baseline open-light photo-current noise measurement was made. The device package was then carefully sliced in half, thus removing the integral lens and the noise measurement was repeated. Figure 23 shows the results for these two configurations.

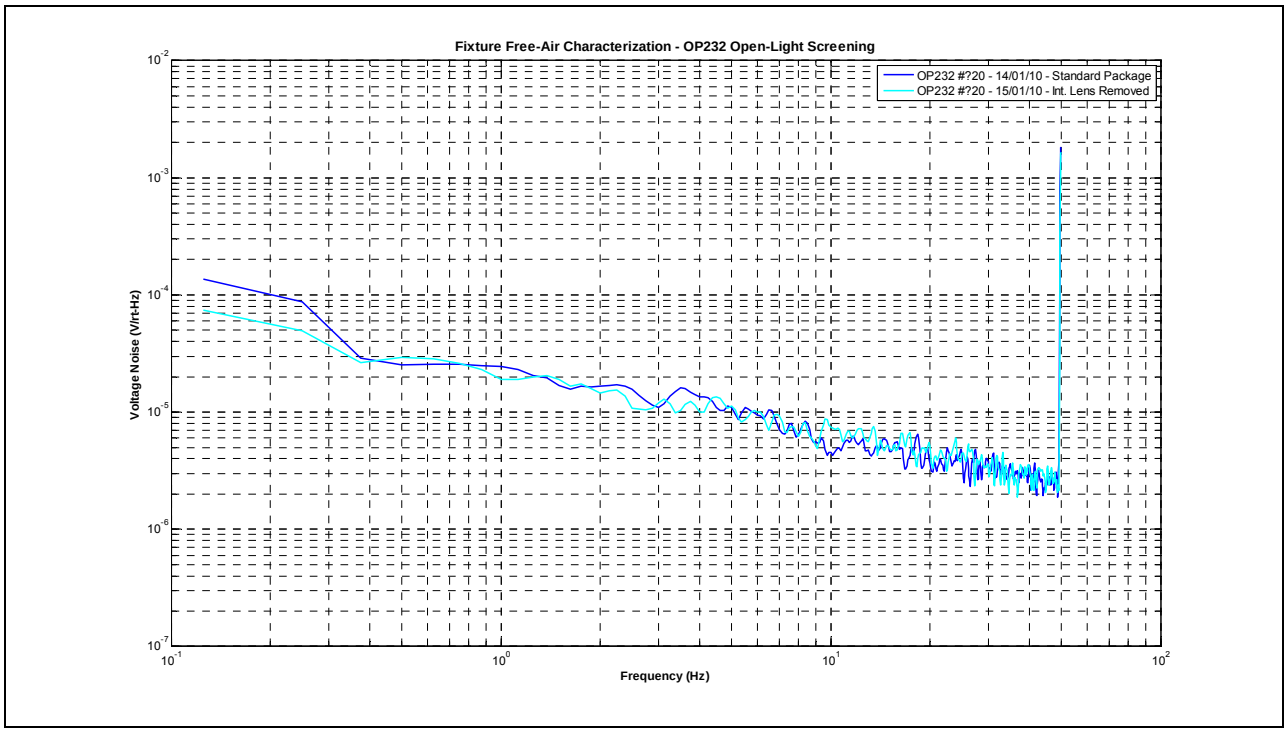

Figure 23. Photo-current Noise for Standard IRLED Package vs Package with Lens Removed.

It can be seen from Figure 23 that there is no difference in the noise behavior of the device; hence there is no dependence on the location or even the existence of the internal lens. This result shows that the source of the excess noise is fundamental in nature and resides within the silicon chip / active area of the IRLED.

A number of sample devices were scraped perfecting a technique for slicing the package in half. However, a quick visual inspection highlighted a significant difference in the appearance of the active area from device-to-device. A few of these units were inspected in more detail under a digital microscope. Figure 24 (left) shows an image of a scrap OP232 device with a generous amount of epoxy covering the chip and bridging the cathode to the case. Figure 24 (right) shows OP232 #020 which exhibited high photo-current noise.

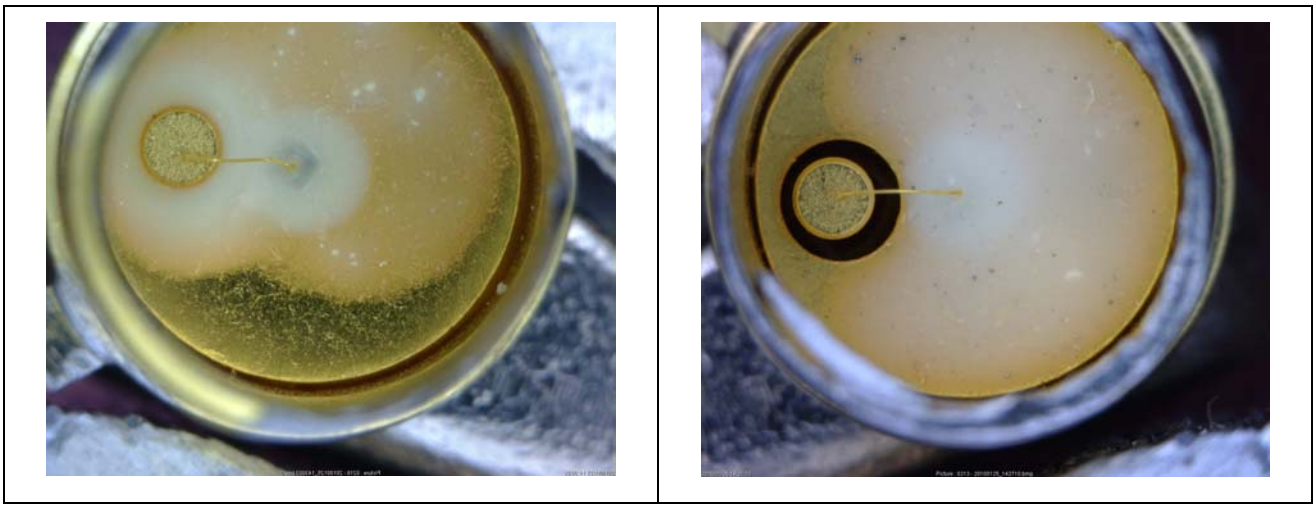

Figure 24. Dissections Through IRLED Packages (left) Scrap OP232 (right) OP232 #020 High Photo-current Noise.

For comparison, a very low noise OP232 device was dissected. Figure 25 (left) shows the distribution of epoxy for a device that exhibits low photo-current noise. It can be seen that the amount and distribution of epoxy is quite different to the high noise case. Also, there is a visible difference in the thickness/transparency of the epoxy layer each device too. This provides some indication that there may a relation between the amount/distribution/transparency of the epoxy and the photo-current noise of the device. Unfortunately these characteristics of the epoxy can only be fully observed under destructive tests, which I don't intend to pursue further at this stage.

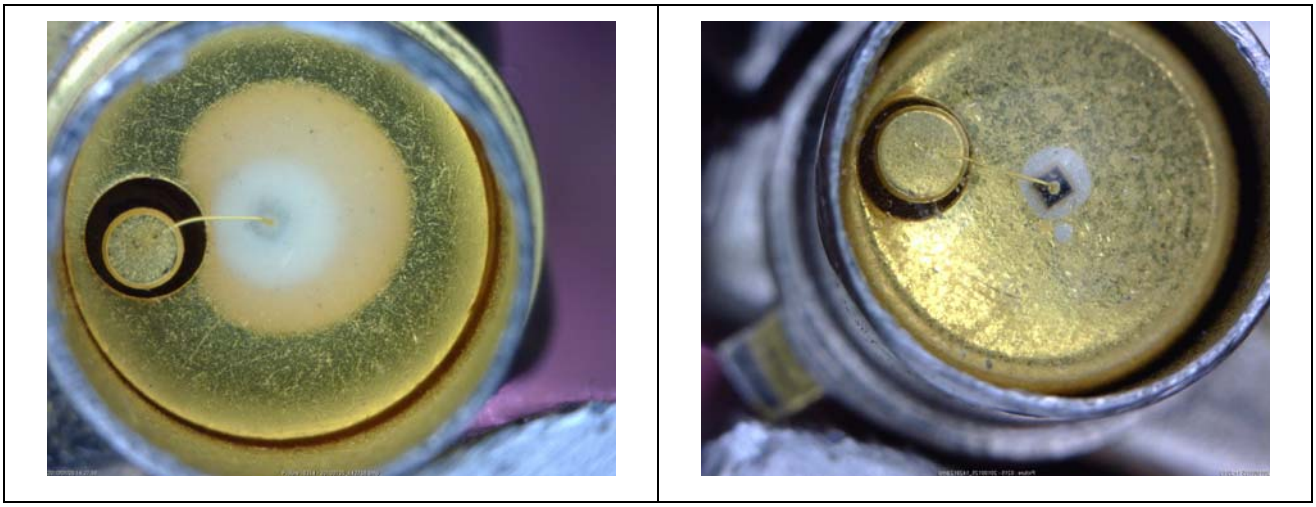

Figure 25. Dissections Through IRLED Packages (left) OP232 #013 Very Low Photo-current Noise (right) Vishay TSTS7100 device.

The variations in the amount and distribution of epoxy we observed was a surprise, given that I would have assumed the operation would be part of a controlled manufacturing process. The OP232's were originally selected as the culmination of a sensor study conducted by ourselves and our collaborator, Nick Lockerbie at the University of Strathclyde. At that time (~2004) these represented the best devices available on the market for this application. However, I have recently sought more state-of-the-art devices, from alternative manufacturers for comparison. I identified the Vishay TSTS7100 as equivalent to the OP232. The opto-mechanical properties are essentially identical. However, the electrical properties differ, for example the pin-outs are reversed and the TSTS7100 has a much larger forward current handling capability than the OP232 (250mA and 100mA respectively).

Figure 25 (right) shows the dissection through the TSTS7100 device. It can be seen that the amount and distribution of epoxy is quite different compared to its OP232 counterpart. The following section provides the results of photo-current noise measurements made on these alternative IRLEDs.

5.9 Alternative IRLED (Vishay TSTS7100)

A large quantity of these devices were procured (~2000) and we noted that they came from different production batches. The open-light photo-current noise was measured for a random sample of devices from each of these batches. Figure 26 illustrates the distribution of open-light photo-current noise measurements for the batch denoted 909 (production date, week 9 of 2009).

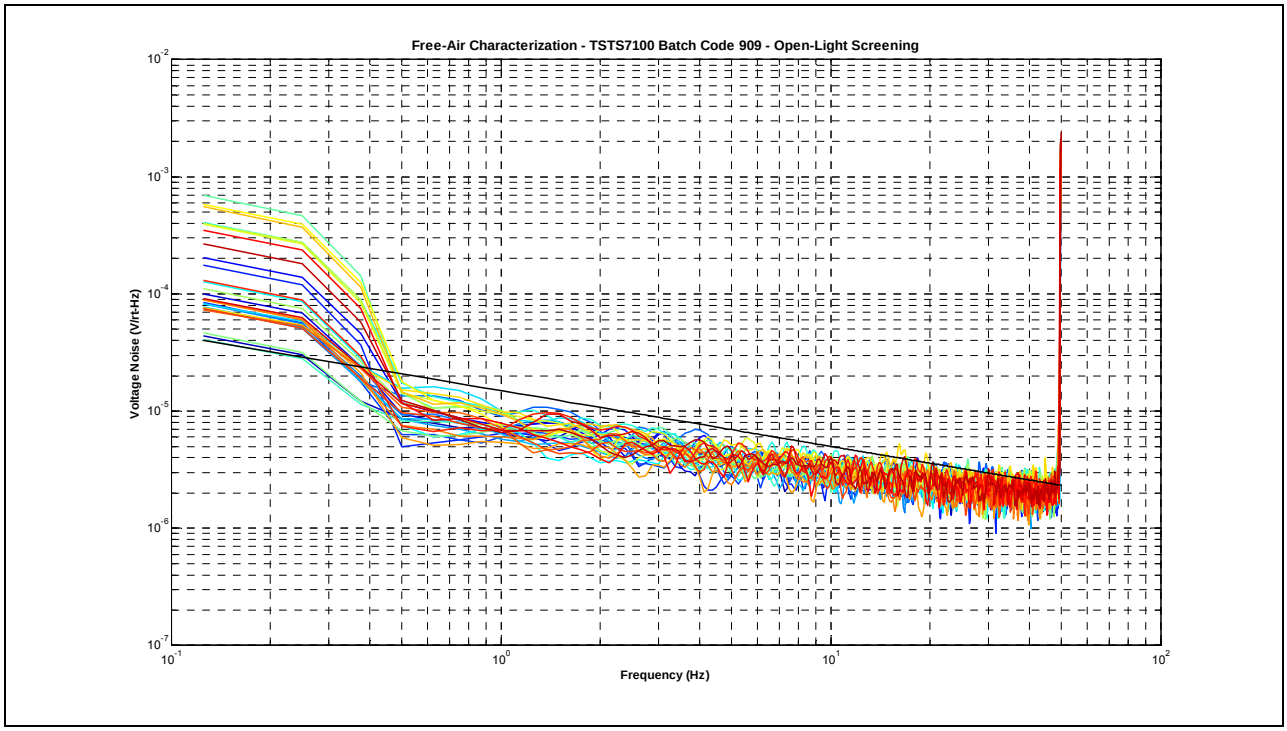

Figure 26. Alternative IRLED (Vishay TSTS7100) Batch 909 Open-light Photo-current Noise Results.

Figure 27 illustrates the distribution of open-light photo-current noise measurements for the batch denoted 940 (production date, week 40 of 2009).

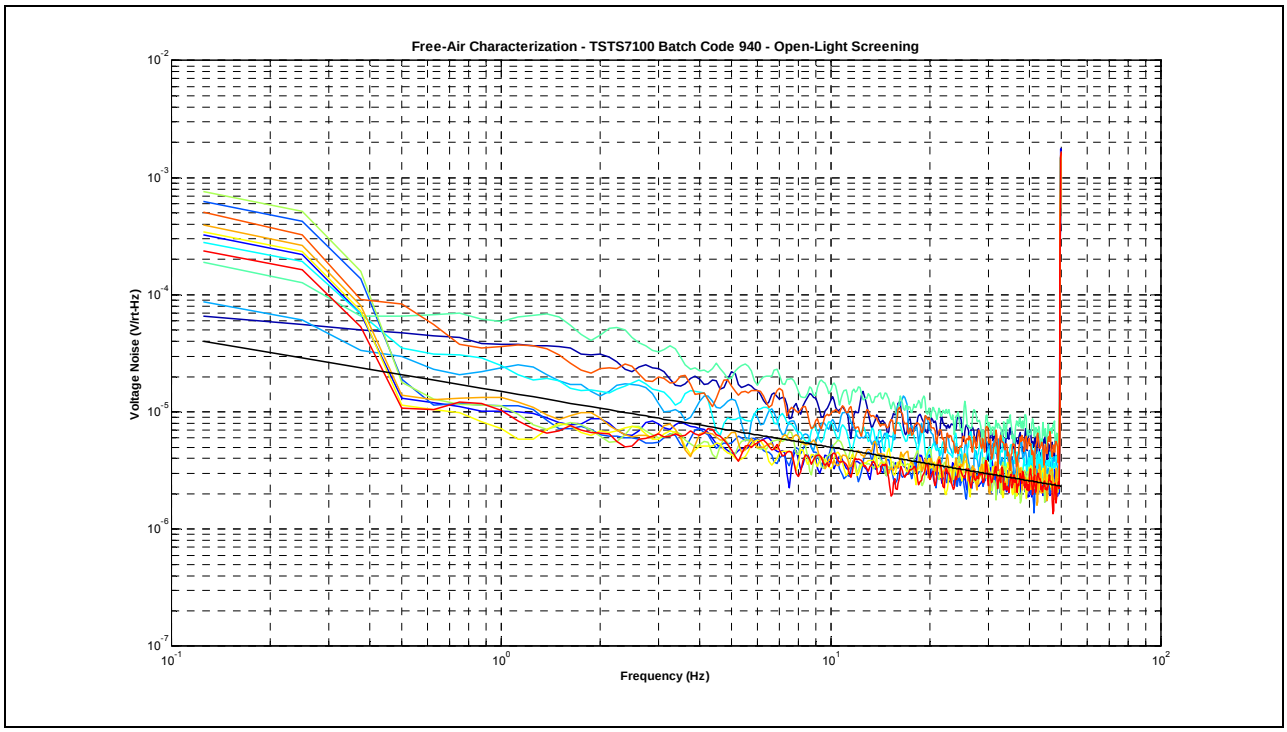

Figure 27. Alternative IRLED (Vishay TSTS7100) Batch 940 Open-light Photo-current Noise Results.

Finally, Figure 28 illustrates the distribution of open-light photo-current noise measurements for the batch denoted 001 (production date, week 1 of 2010).

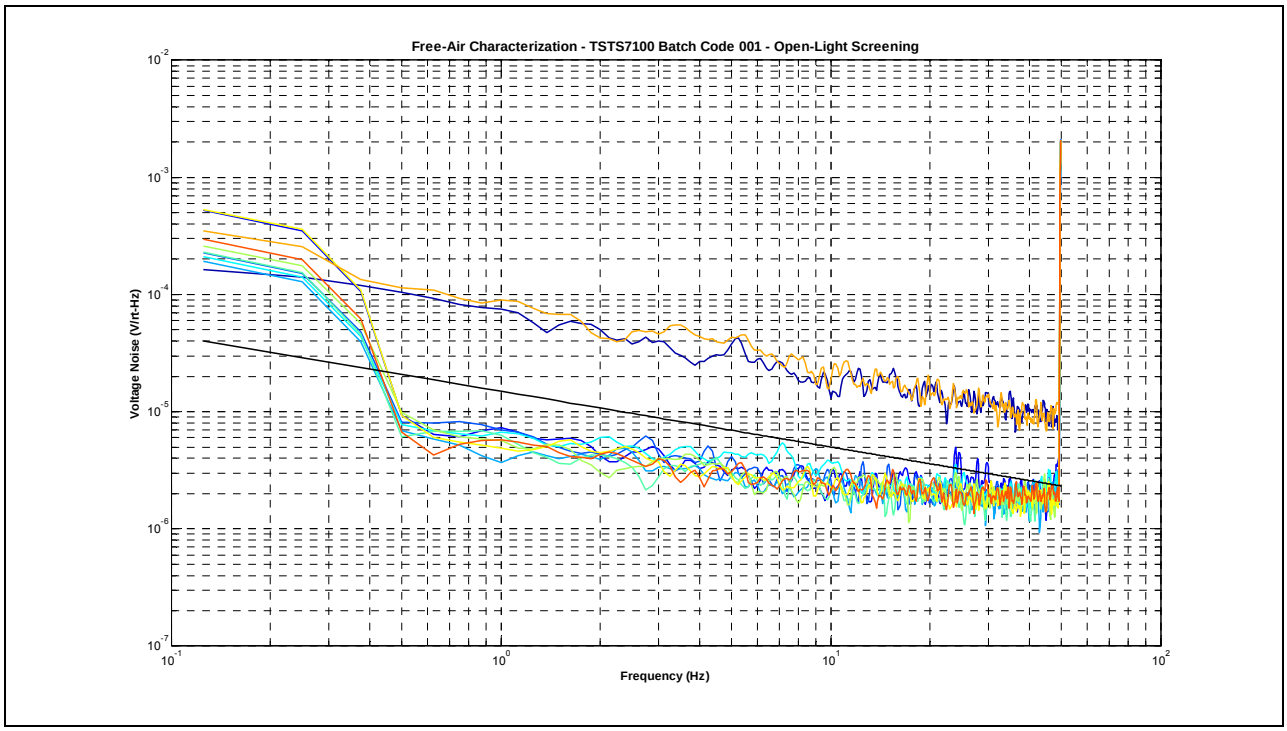

Figure 28. Alternative IRLED (Vishay TSTS7100) Batch 001 Open-light Photo-current Noise Results.

It can be seen from Figures 26, 27 and 28 that there is a variation in the IRLED noise performance from batch-to-batch. For example, batch 909 exhibited a 100% pass rate, batch 940 exhibited a 50% pass rate and finally batch 001 exhibited an 80% pass rate. If we were to proceed with procuring additional units, then these units are certain to come from the most recent 001 batch. We can therefore not expect a 100% pass rate and so additional photo-current noise screening will be required. However, the alternative TSTS7100 devices look a great deal more promising, providing us with a significantly higher yield than with the OP232's.

6 Conclusions and First 50 Full Characterization Results

The noise measurements presented herein provide overwhelming evidence that the IRLED is the source of the excess noise measured in the production BOSEMs. Given that the excess noise has also been found to be present in the NPOSEMs demonstrates that none of the subsequent cleaning or bake-out procedures are responsible for generating the excess noise.

It was determined that due to device-to-device variations in photo-current noise only 10% of the OP232 IRLEDs meet the noise requirement. Screening approximately 700 already assembled BOSEMs to identify which units meet the requirement and which do not, would not be viable on the timescale of the project. In addition, to screen potentially around 7000 IRLEDs to identify those candidates that could be retro-fitted into a BOSEM, would be time consuming and an undesirable route forward.

Fortuitously, during the course of these excess noise investigations, we indentified a viable alternative candidate to the OPTEK OP232 device. The Vishay TSTS7100 is essentially an equivalent IRLED, but we have observed a significantly higher pass rate for these devices. There is some batch-to-batch variation in pass rates, ranging from 100%, down to 50% in the worst case. We therefore proposed that the TSTS7100 IRLED's should be screened for photo-current noise and the successful devices be retro-fitted into the already assembled BOSEMs, replacing the original OP232 IRLED.

UHV qualification for these alternative IRLEDs has been sought and approval has been given to use these devices in the aLIGO vacuum. MTTF data has also been provided by the manufacture and passed on to the aLIGO project management, which has raised no concerns.

We wished to attempt a trial run, installing the newly approved TSTS7100 IRLEDs into 50 in-process spare BOSEMs that still had to be assembled. A sufficient quantity of TSTS7100 would be screened for photo-current noise, burned-in, cleaned and baked, using exactly the same procedures outlined for the original OP232 device [2][3]. A minor modification is required to the MACOR IRLED sleeve (D060116) so that it can accommodate the TSTS7100 IRLED. This is due to the polarity of the pins being reversed on the TSTS7100 compared to the OP232. The modification allows the IRLED to be rotated through 180 degrees, thus ensuring that the pin-outs correctly mate-up with those on the flexi-circuit.

The IRLEDs are to be screened in batches of 55 units, where I have outlined a noise screening procedure to be followed in-house at Birmingham [see Appendix A]. Birmingham technicians will conduct the 1st pass of the IRELD screening process and present me with data traces for the 55 units. I then plot and interrogate these traces to ensure that they meet the requirement at all frequencies across the band of interest. Figure 29 shows the raw spectra for each IRLED device. It can be seen that each device meets the requirement at 10 Hz. However, in some cases external environmental noise can be seen to be coupling in. Above 10 Hz mains peaks and harmonics thereof, can be observed. We also have a lot of demolition/building work going on in close proximity on campus and this can couple in at frequencies below 10 Hz.

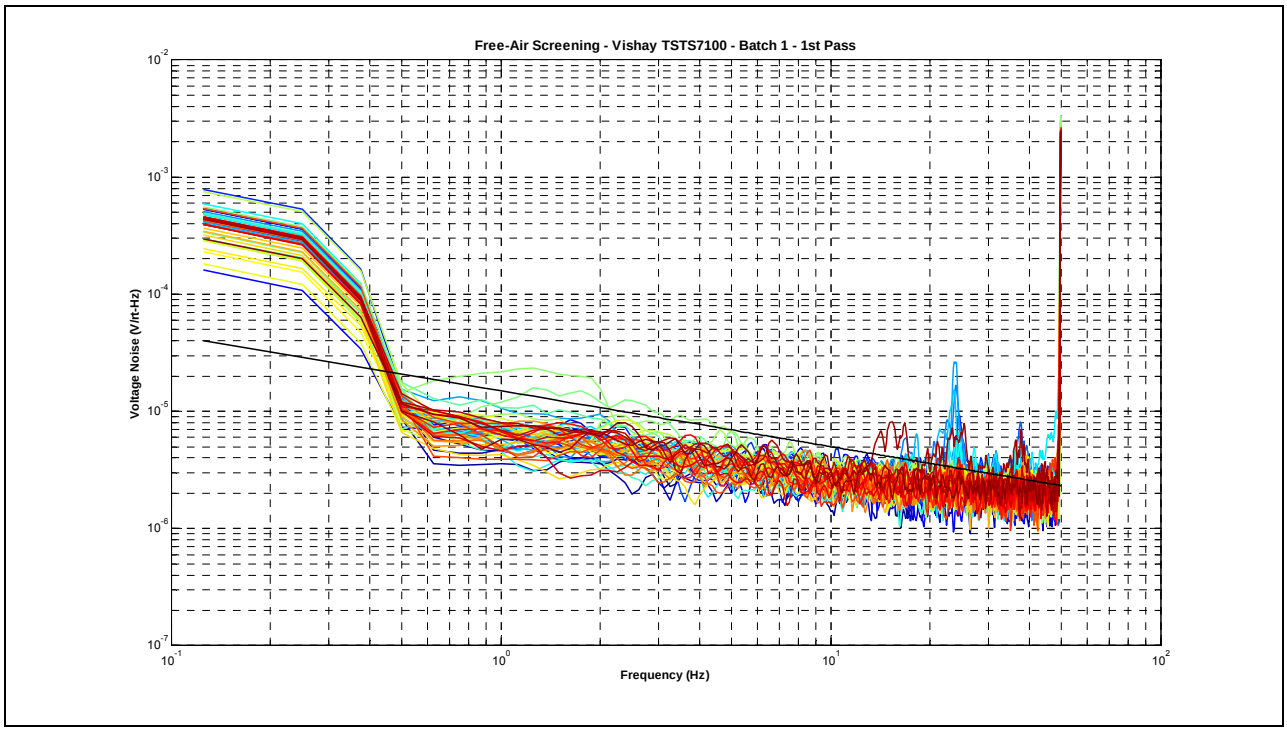

Figure 29. IRLED Screening Batch 1 - 1st Pass Results.

I also provide verification checks to ensure that no traces are missing, duplicated or otherwise erroneous. In the event of excess environmental noise coupling into the measurements, I will then seek to repeat those measurements for that specific IRLED. This will then provide all the data to form the 2nd pass plot and complete the IRLED screening process. At this stage we can be confident that the entire batch of 55 IRLEDs are suitable to be installed into BOSEMs. Figure 30 shows the 2nd pass plot data.

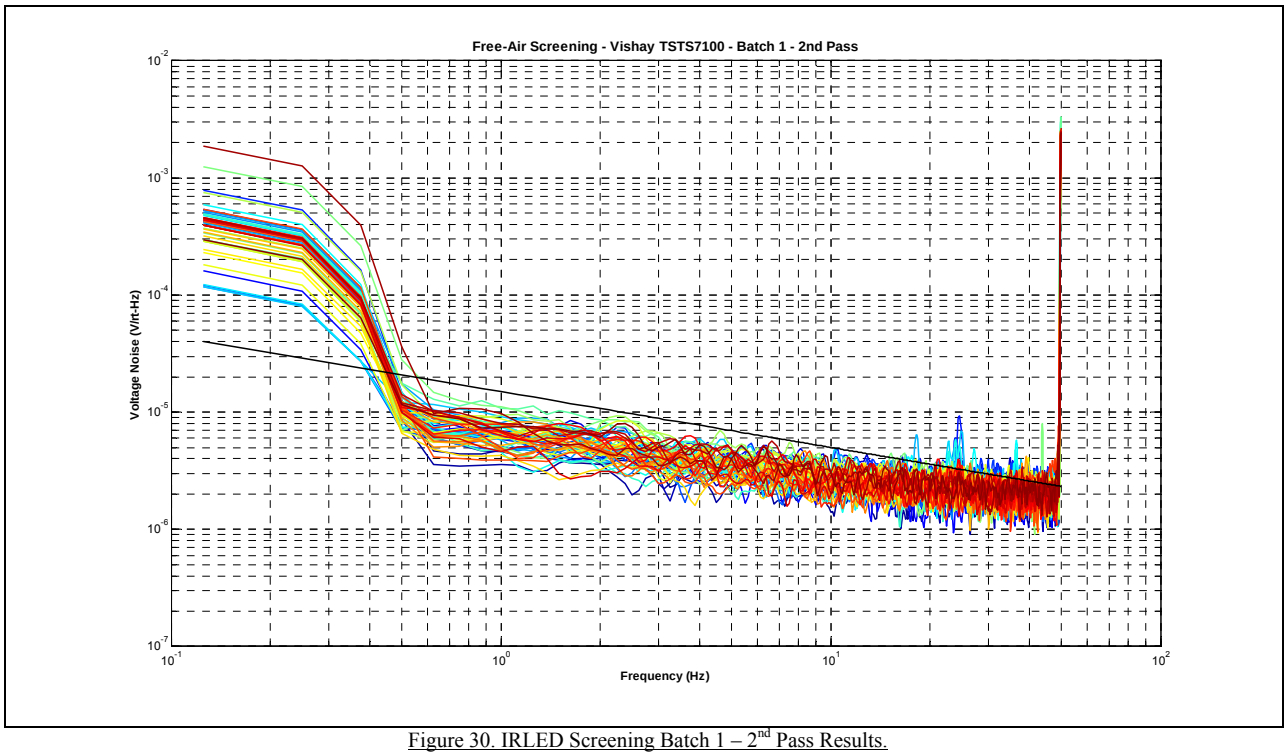

Figure 30. IRLED Screening Batch 1 – 2nd Pass Results.

During the assembly process the final stage is to test the BOSEMs [3]. This is conducted on our Automated Test Equipment (ATE) and provides measurements such as the PD current and transfer ratio. However, for this new batch of 50 BOSEMs is was desirable to prove beyond any doubt that the sensitivity performance would meet the requirement. This would therefore require the full characterization of the complete batch of BOSEM i.e. the responsivity and noise being measured for each of the 50 units. Each BOSEM has been tested in accordance with the procedure detailed previously in Section 2.

Figures 31-35 show the full characterization results for each of the 50 BOSEMs (10 BOSEMs per plot). The black trace in each figure represents the exact performance requirement.

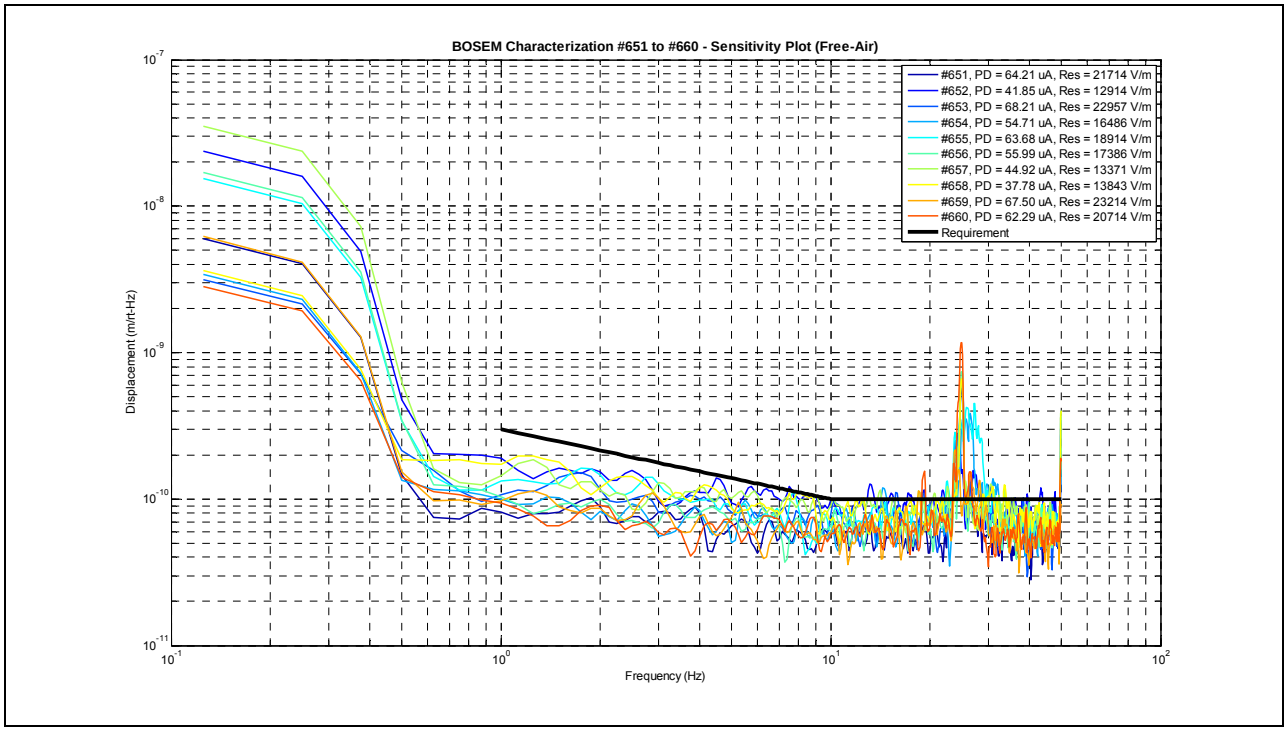

Figure 31. BOSEM #651 to #660 Full Characterization Results.

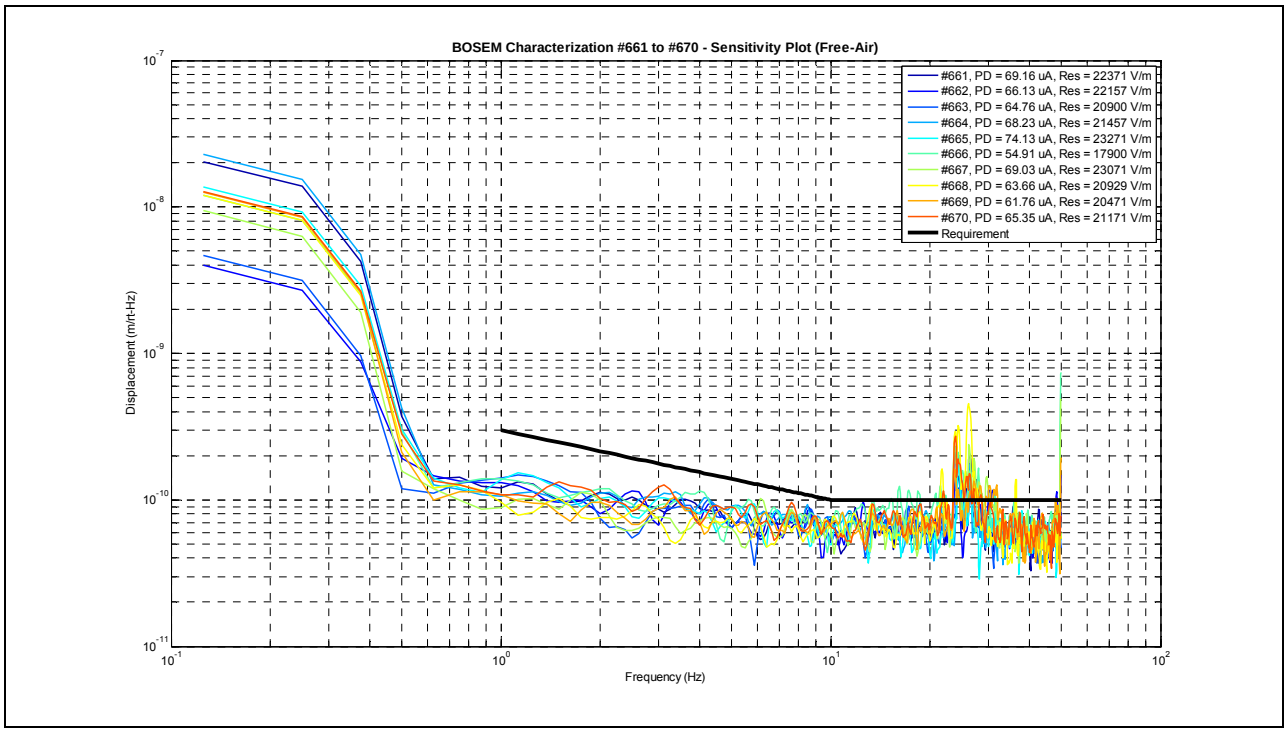

Figure 32. BOSEM #661 to #670 Full Characterization Results.

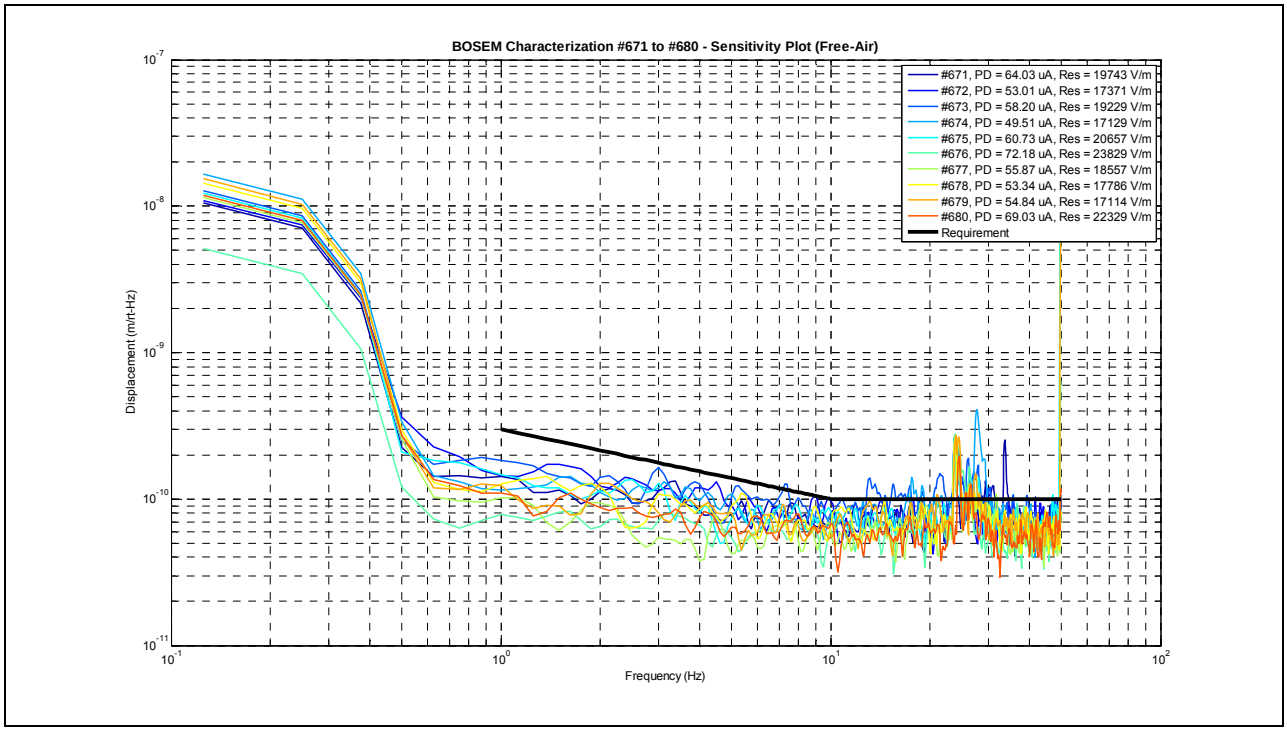

Figure 33. BOSEM #671 to #680 Full Characterization Results.

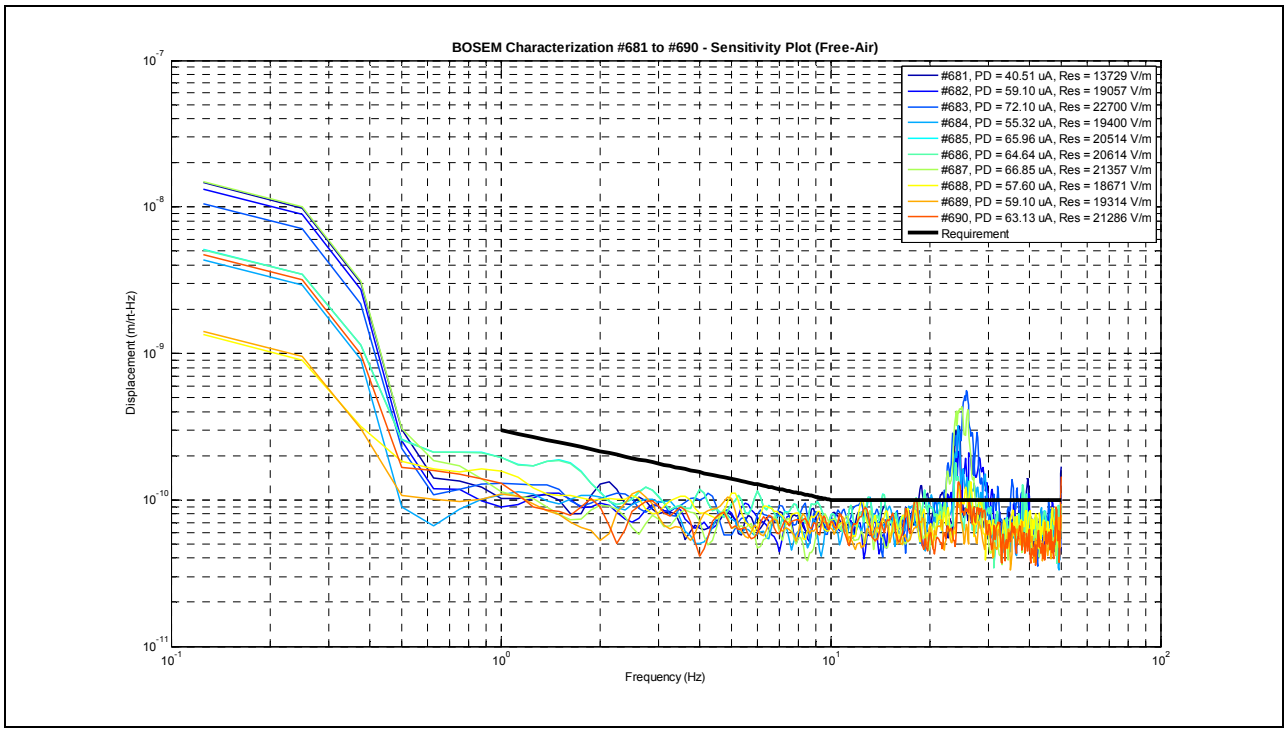

Figure 34. BOSEM #681 to #690 Full Characterization Results.

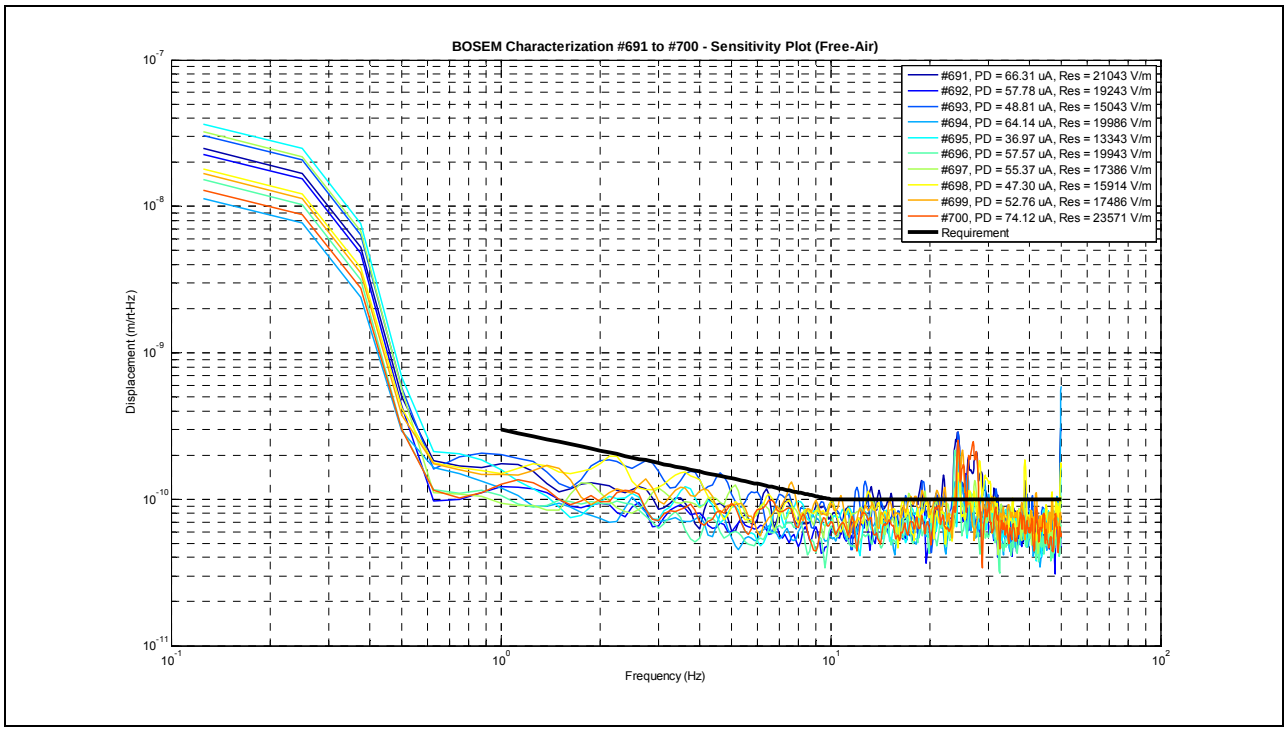

Figure 35. BOSEM #691 to #700 Full Characterization Results.

It can be seen that all the BOSEMs meet the performance requirements (excluding the contribution of environmental noise at mains frequencies). PD currents we found to range from 37 µA up to 74 µA. An acceptable range has since been agreed of 45 µA to 80 µA inclusive. In the event of a PD current being measured out of this range, then the IRLED will be swapped for a spare and re-tested until within range. This should take no more than a single iteration.

The characterization results now show good correlation between the PD current (measured on the ATE) and the Responsivity (measured during the full characterization). This indicates that measuring the PD current during the final stage of assembly using the ATE, would give us confidence in estimating the sensitivity of the BOSEM. However, we would still wish to explicitly verify the performance for a small quantity of samples from each shipment. The USA has requested that we fully characterize 12.5% of all subsequent units we deliver. Our production plan is therefore to proceed with retro-fitting TSTS7100 IRELDs into BOSEMs and deliver these units at a rate of approximately 100 units per month. These units will be tested as follows:-

- 100% of IRLEDs are screened (photo-current noise)
- 100% of BOSEMs are tested by ATE (PD current, transfer ratio and coil parameters etc)
- 12.5% of BOSEMs are fully characterized (responsivity and noise measured)

To identify units that have been fully characterized, a sequential range of serial numbers (#560 - #700) for production BOSEMs (D060218-C) has been defined. n.b. 10 BOSEMs with serial numbers #601 - #608, #579 and #586, are out of circulation as they are employed in tip-tilt stages.

7 Production BOSEM Full Characterization Results

Following are sensitivity performance plots from the remaining production BOSEMs (~12.5%):-

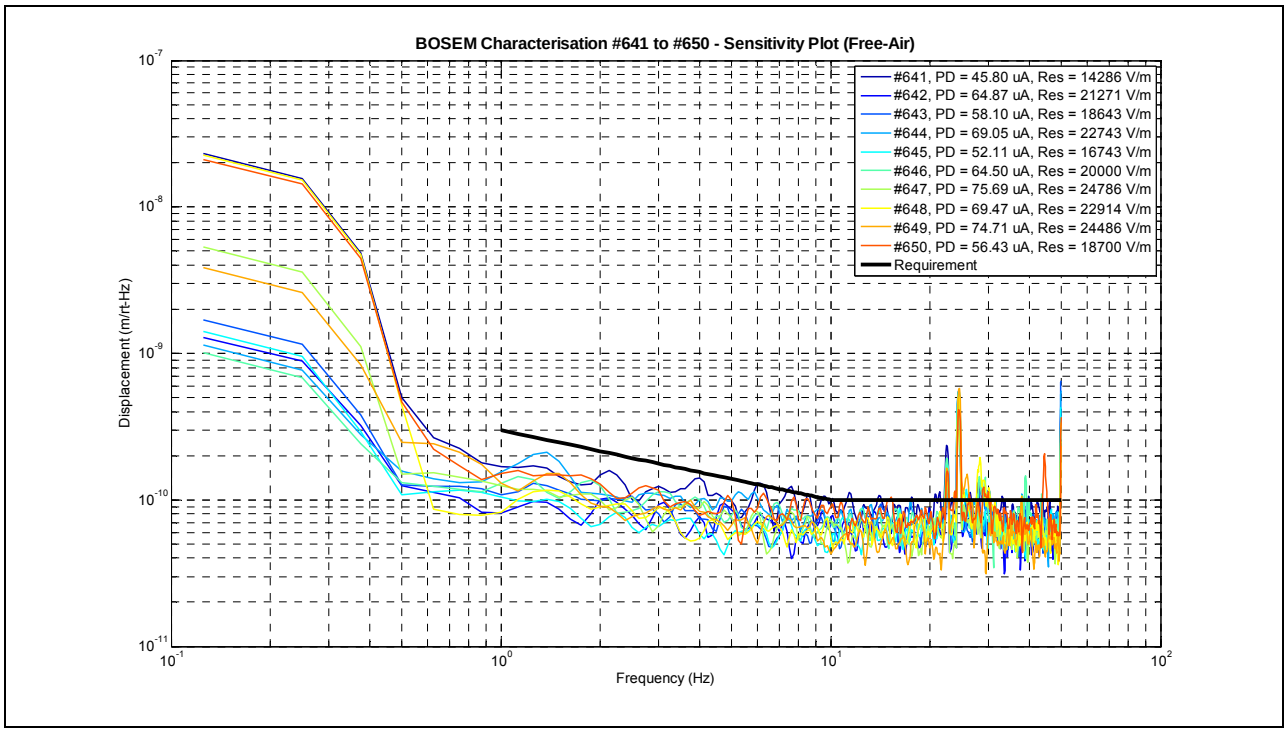

Figure 36. BOSEM #641 to #650 Full Characterization Results.

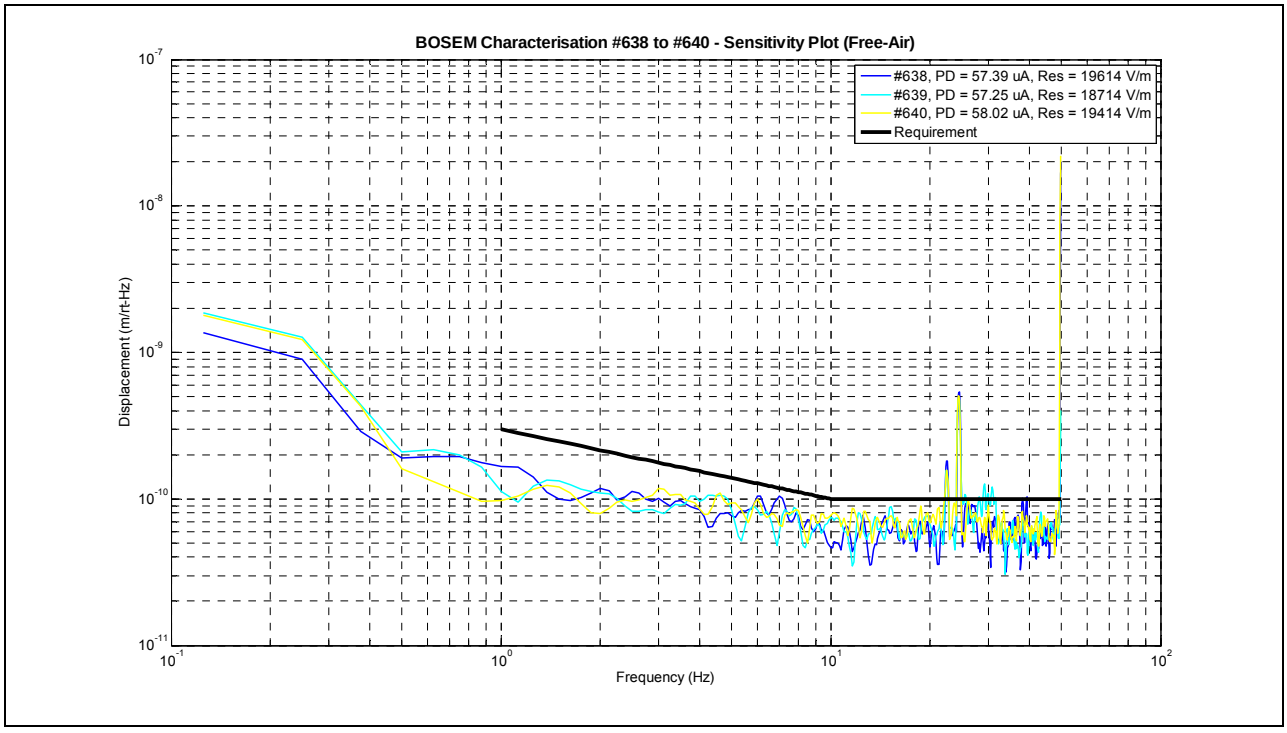

Figure 37. BOSEM #638 to #640 Full Characterization Results.

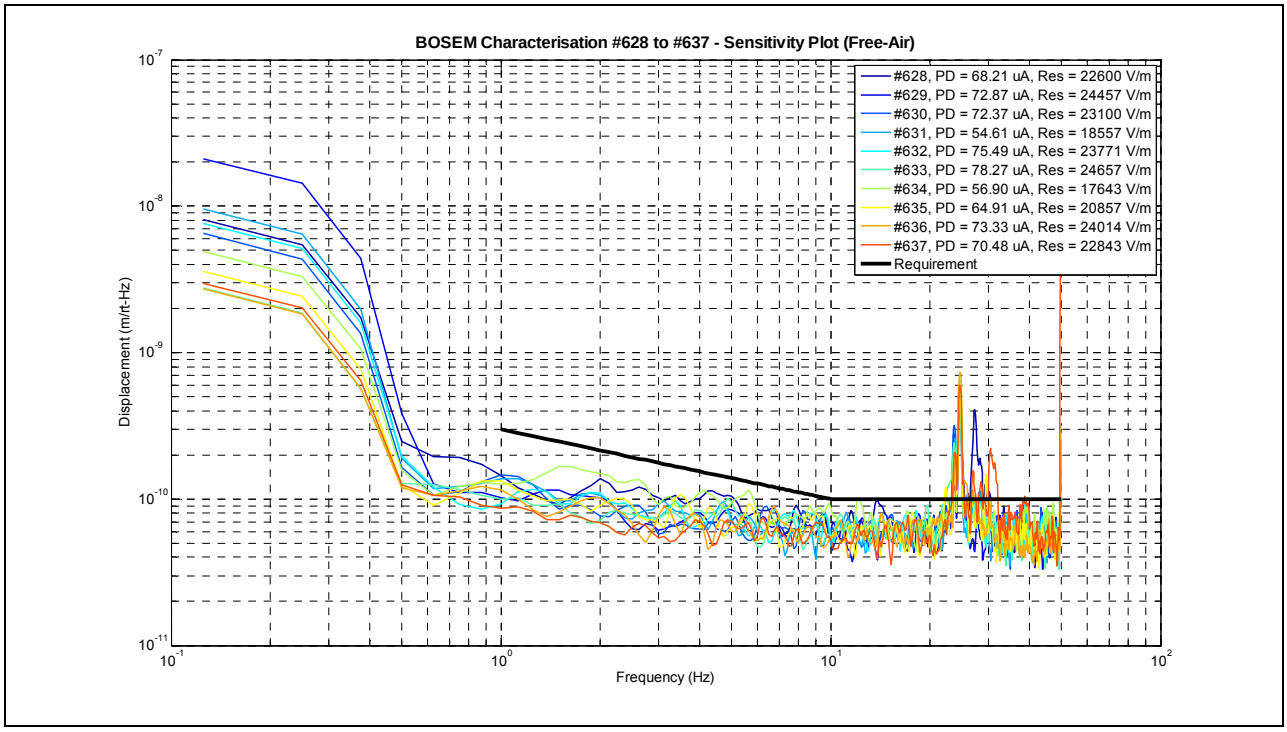

Figure 38. BOSEM #628 to #637 Full Characterization Results.

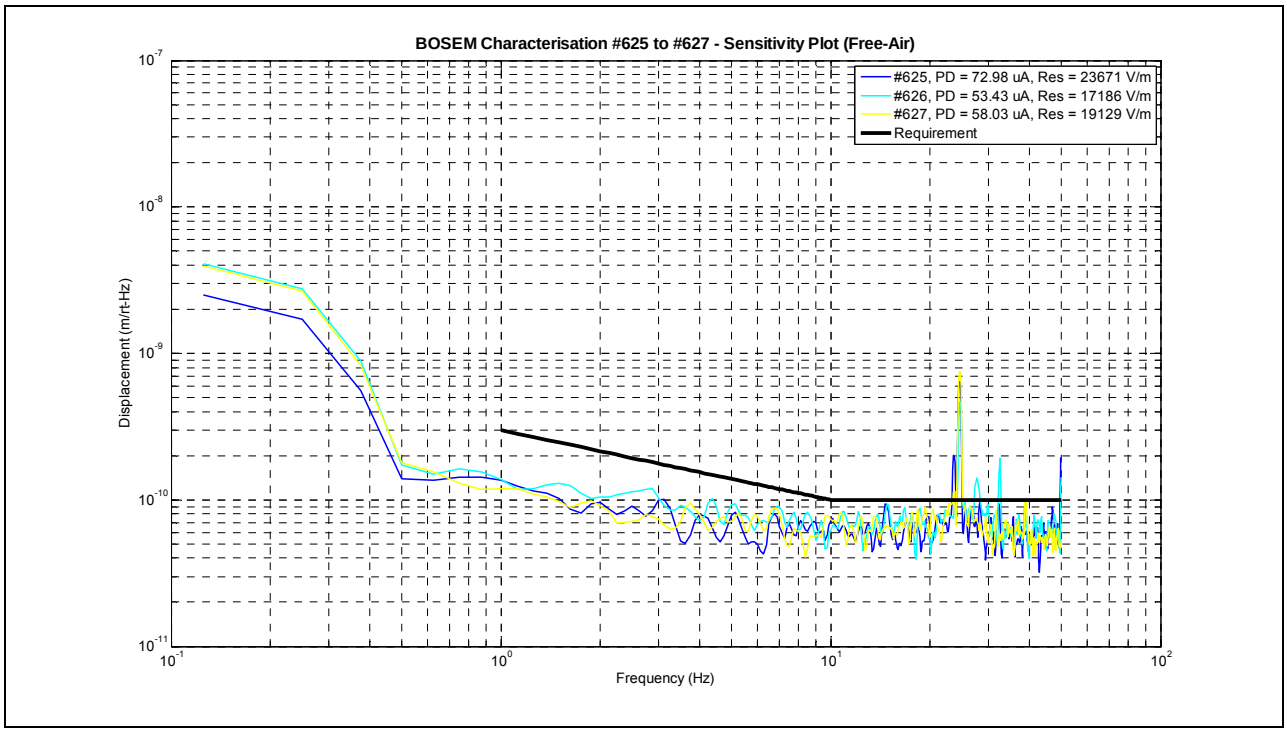

Figure 39. BOSEM #625 to #627 Full Characterization Results.

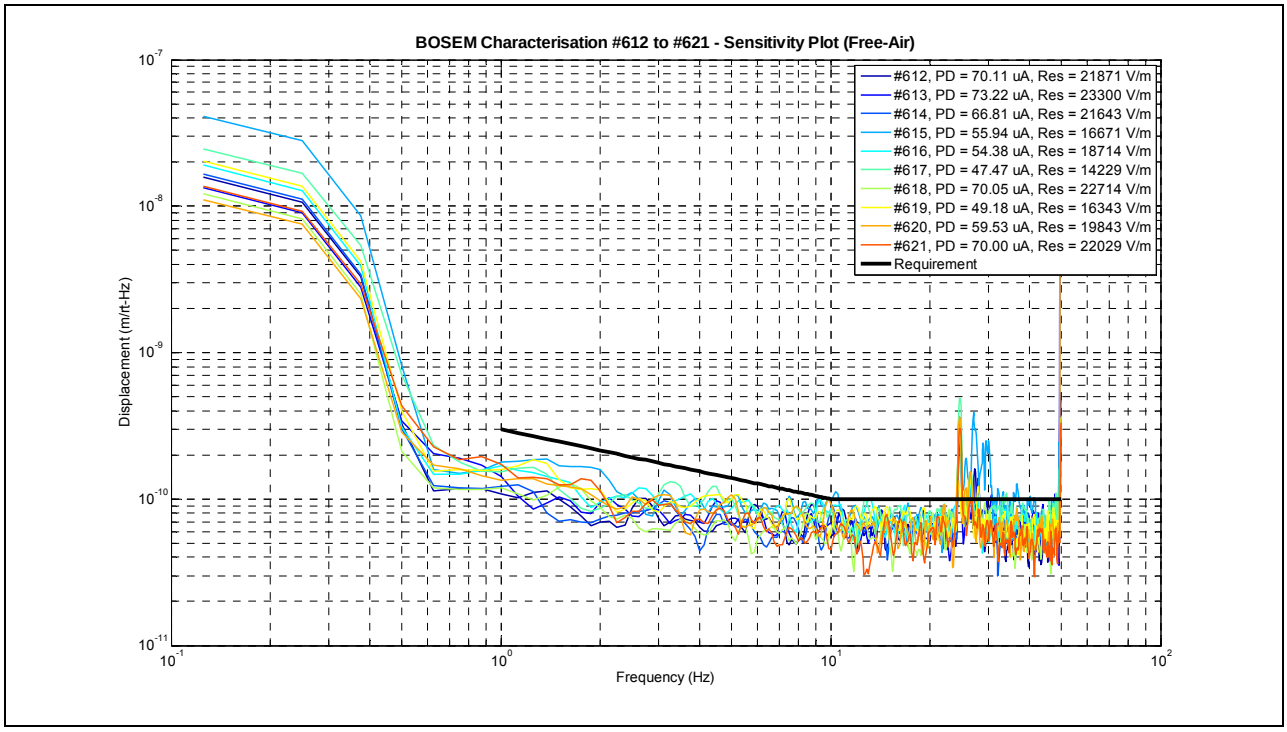

Figure 40. BOSEM #612 to #621 Full Characterization Results.

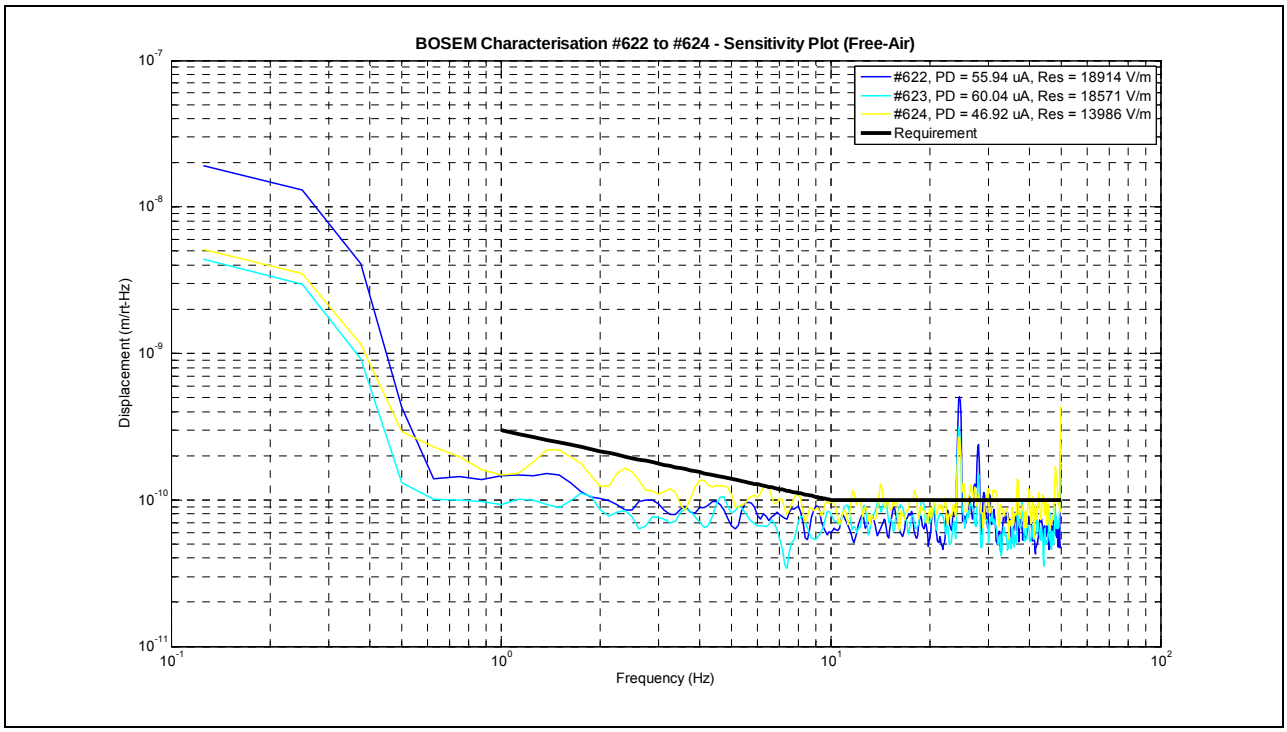

Figure 41. BOSEM #622 to #624 Full Characterization Results.

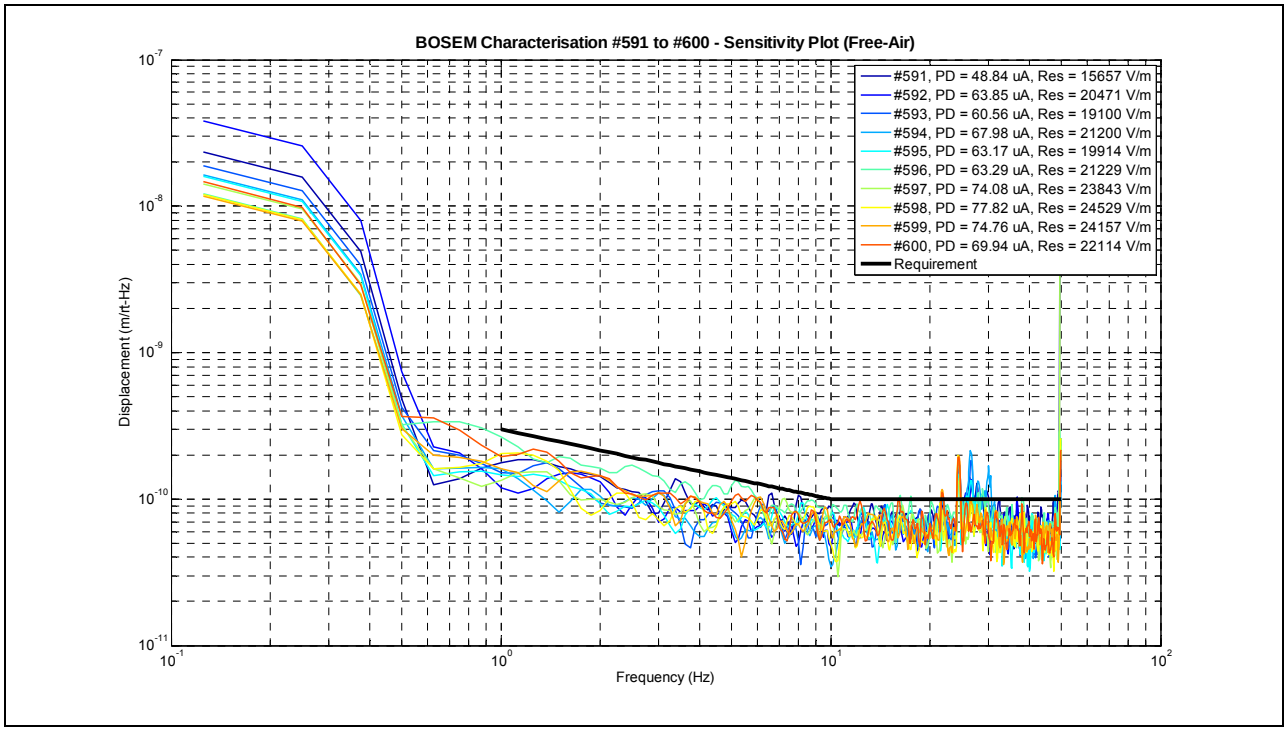

Figure 42. BOSEM #591 to #600 Full Characterization Results.

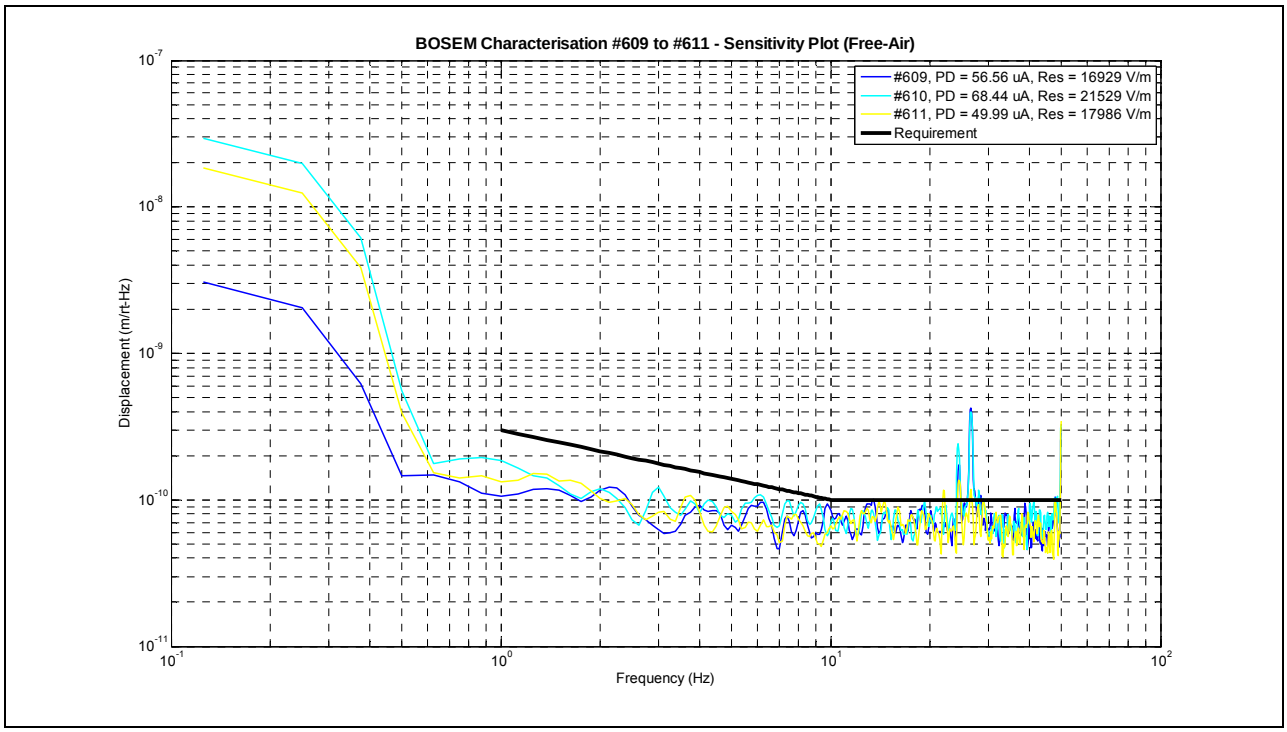

Figure 43. BOSEM #609 to #611 Full Characterization Results.

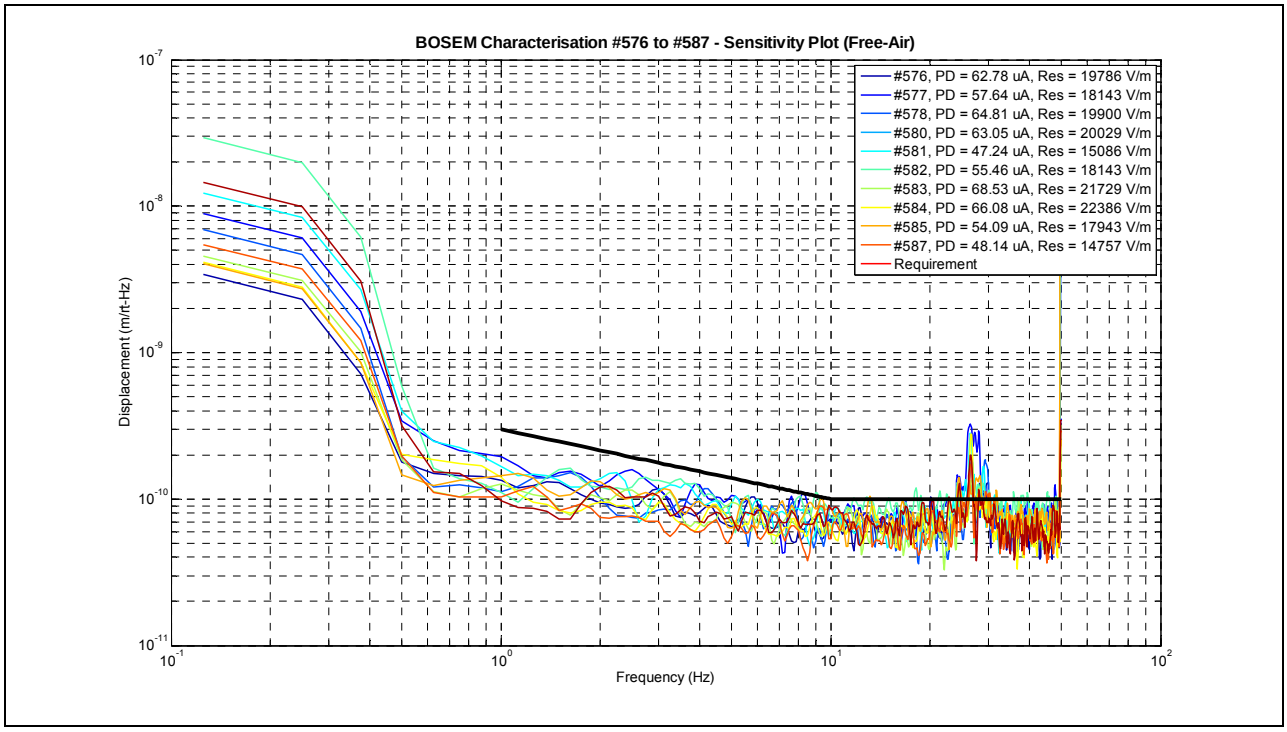

Figure 44. BOSEM #576 to #587 Full Characterization Results.

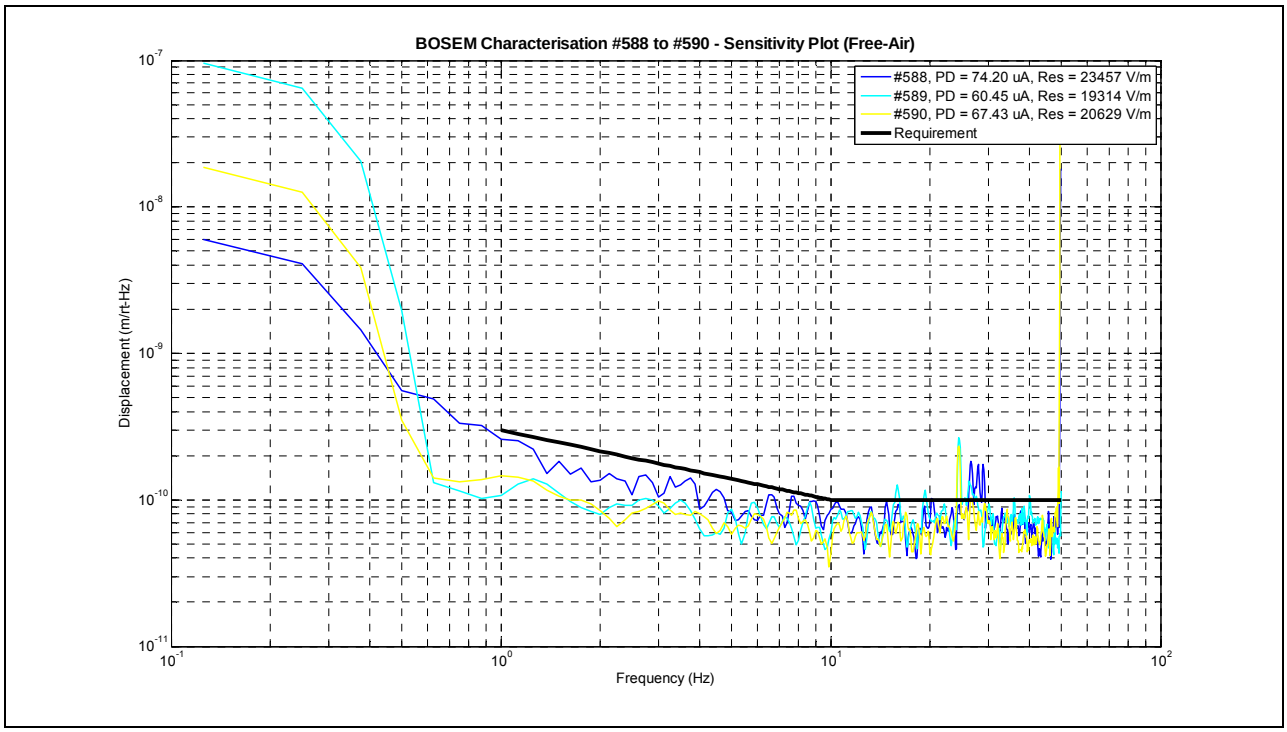

Figure 45. BOSEM #588 to #590 Full Characterization Results.

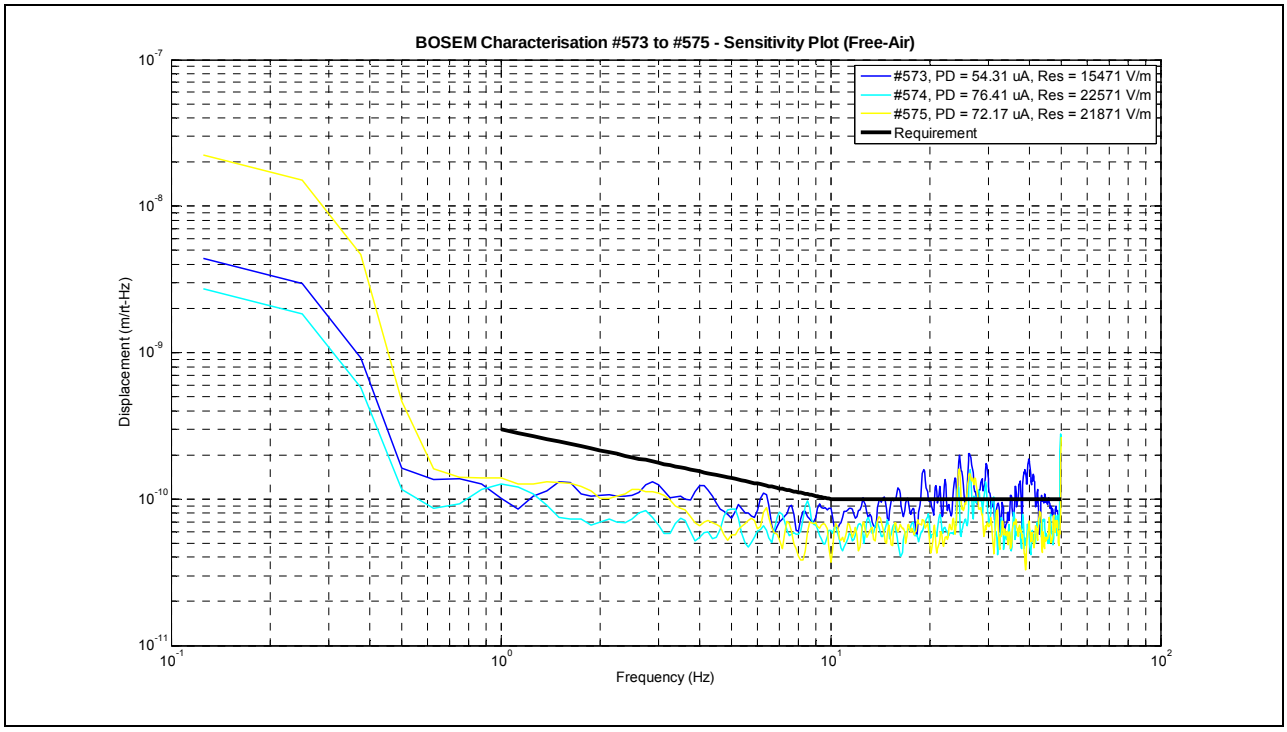

Figure 46. BOSEM #573 to #575 Full Characterization Results.

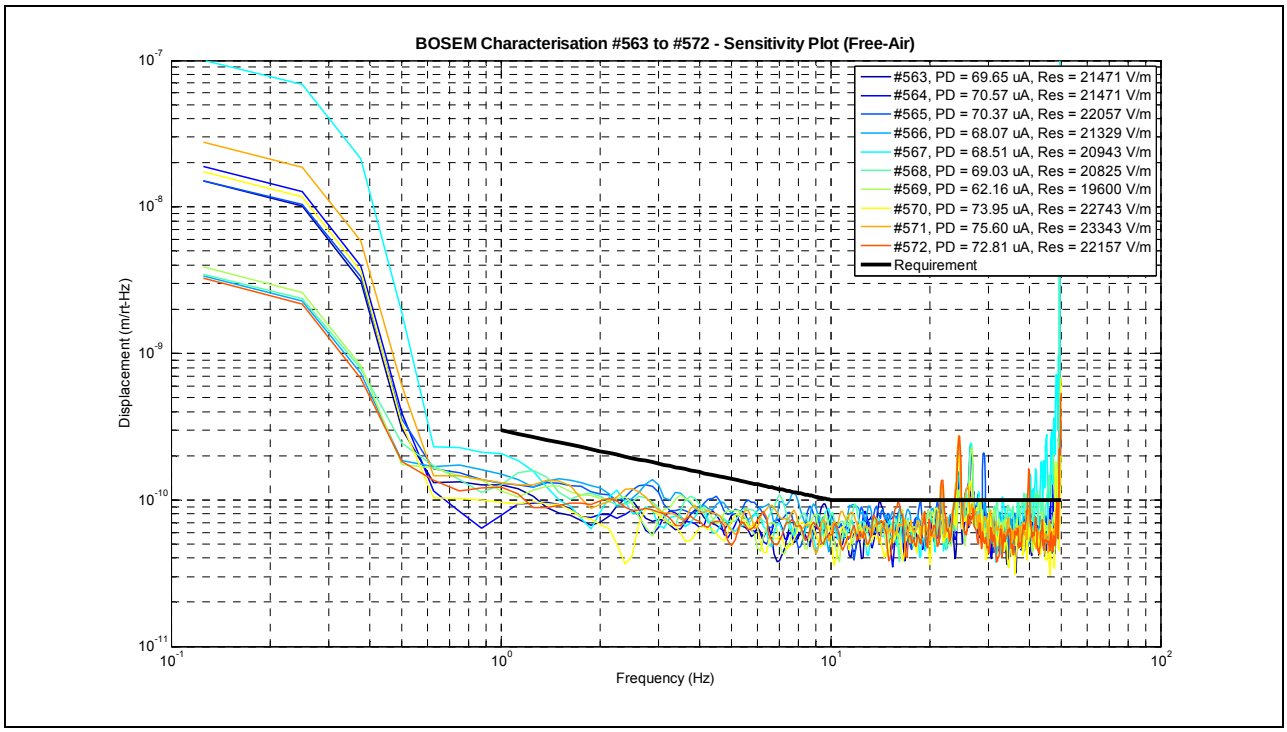

Figure 47. BOSEM #563 to #572 Full Characterization Results.

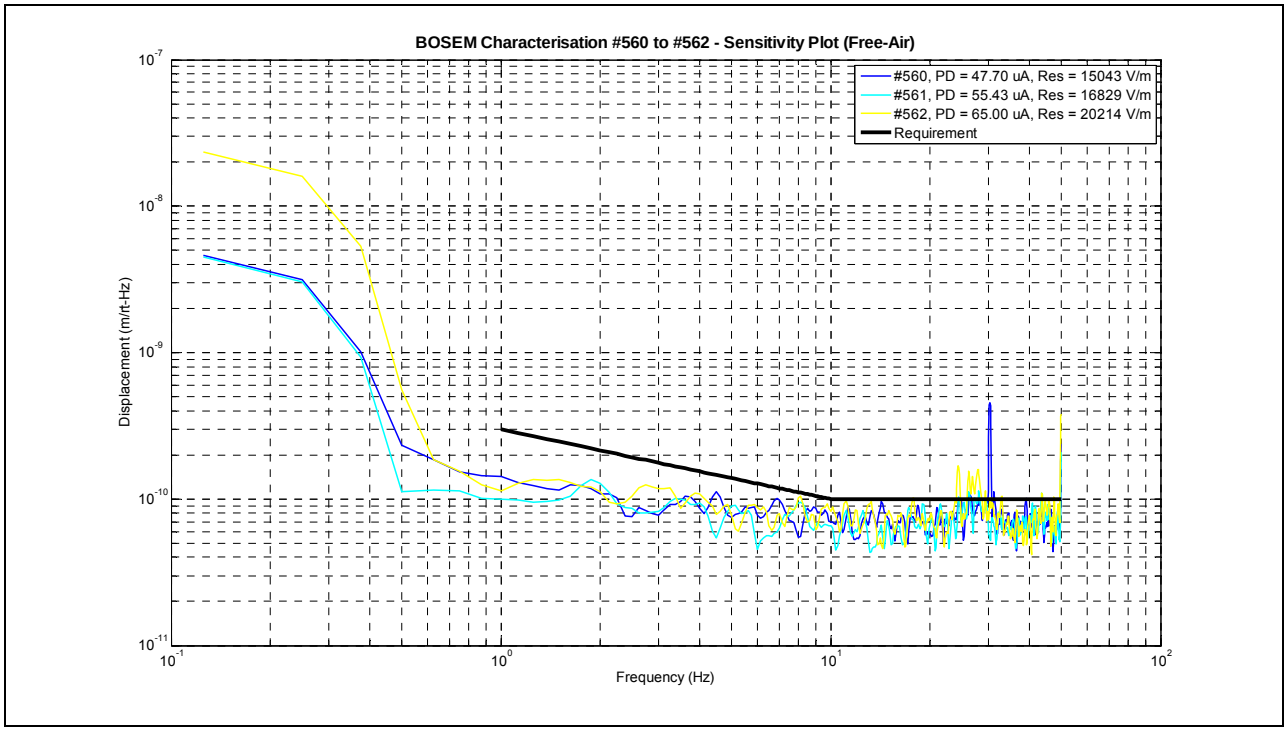

Figure 48. BOSEM #560 to #562 Full Characterization Results.

As can be seen from figures 36-48, all of the production BOSEMs characterized have been observed to meet the sensitivity requirements. Thus demonstrating that the IRLED photo-current noise screening has been successful.

8 Production BOSEM Automated Test Equipment Results

Interrogation of BSOEM ATE data files to observe distributions of measured parameters:-

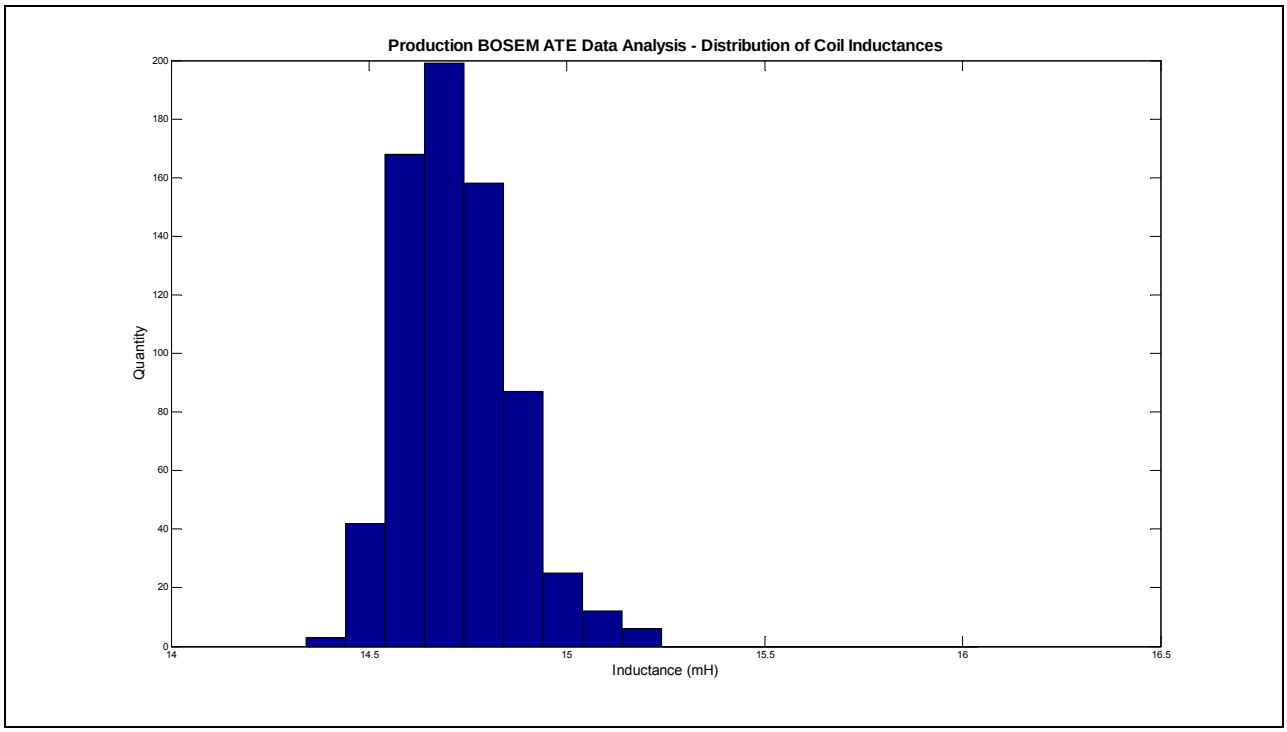

Figure 49. Production BOSEM ATE Data Analysis - Distribution of Coil Inductances.

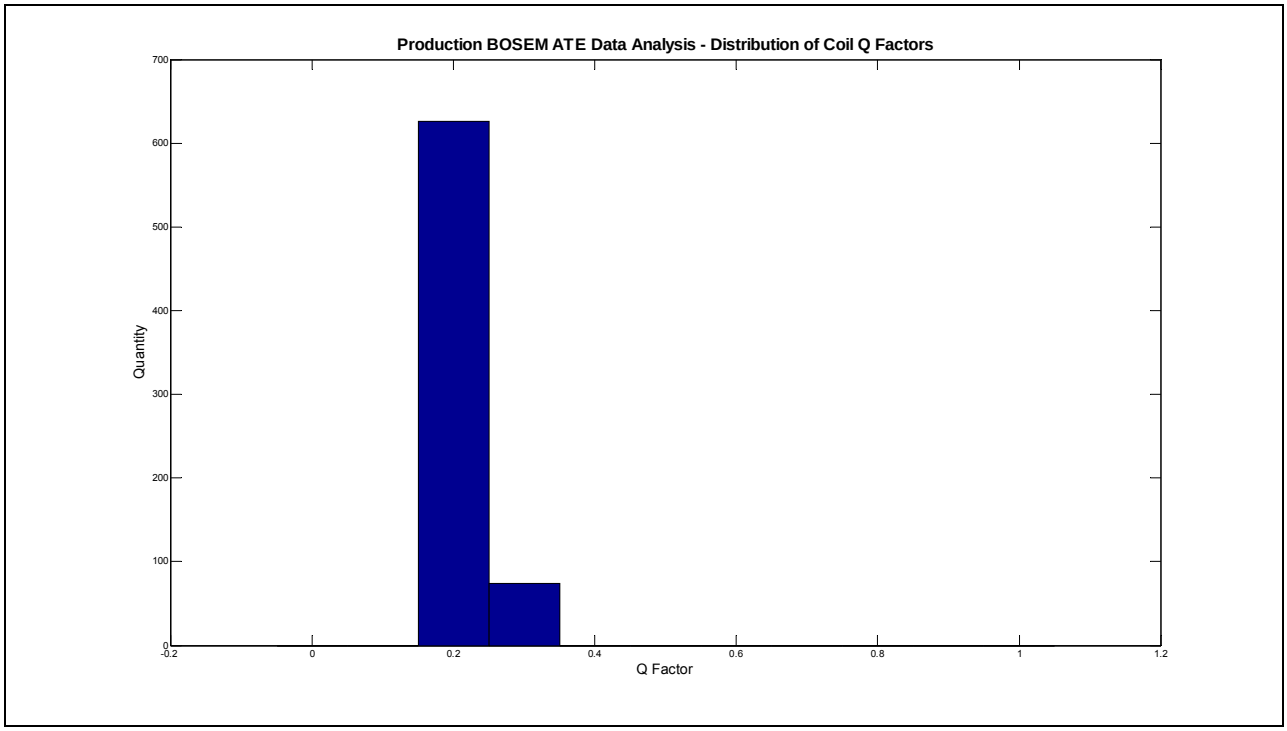

Figure 50. Production BOSEM ATE Data Analysis - Distribution of Coil Q Factors.

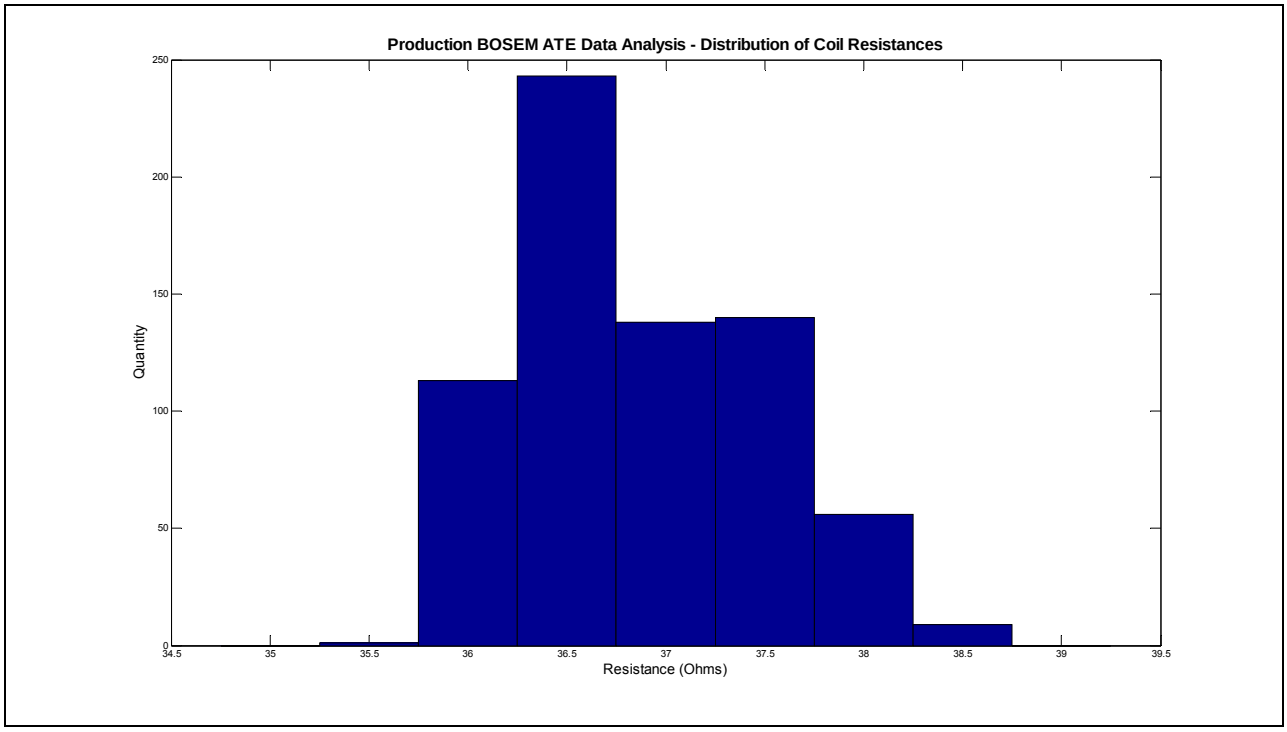

Figure 51. Production BOSEM ATE Data Analysis - Distribution of Coil Resistances.

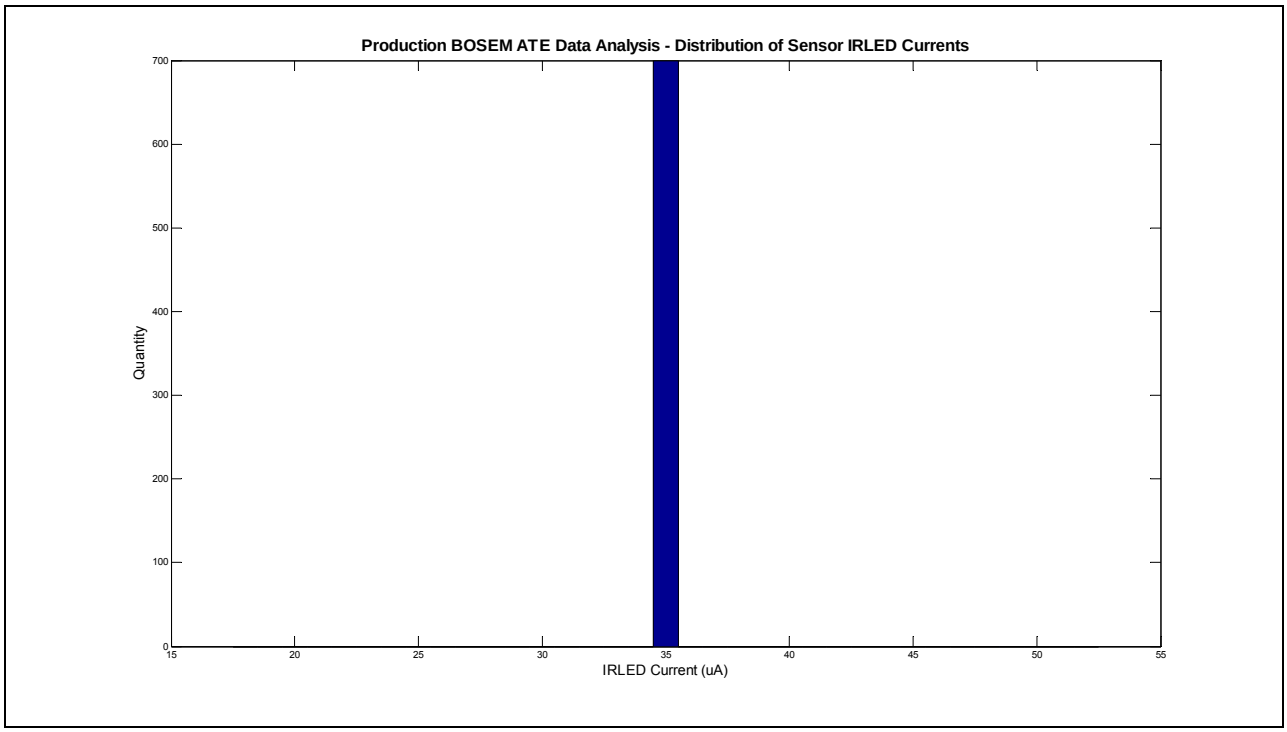

Figure 52. Production BOSEM ATE Data Analysis - Distribution of Sensor IRLED Currents.

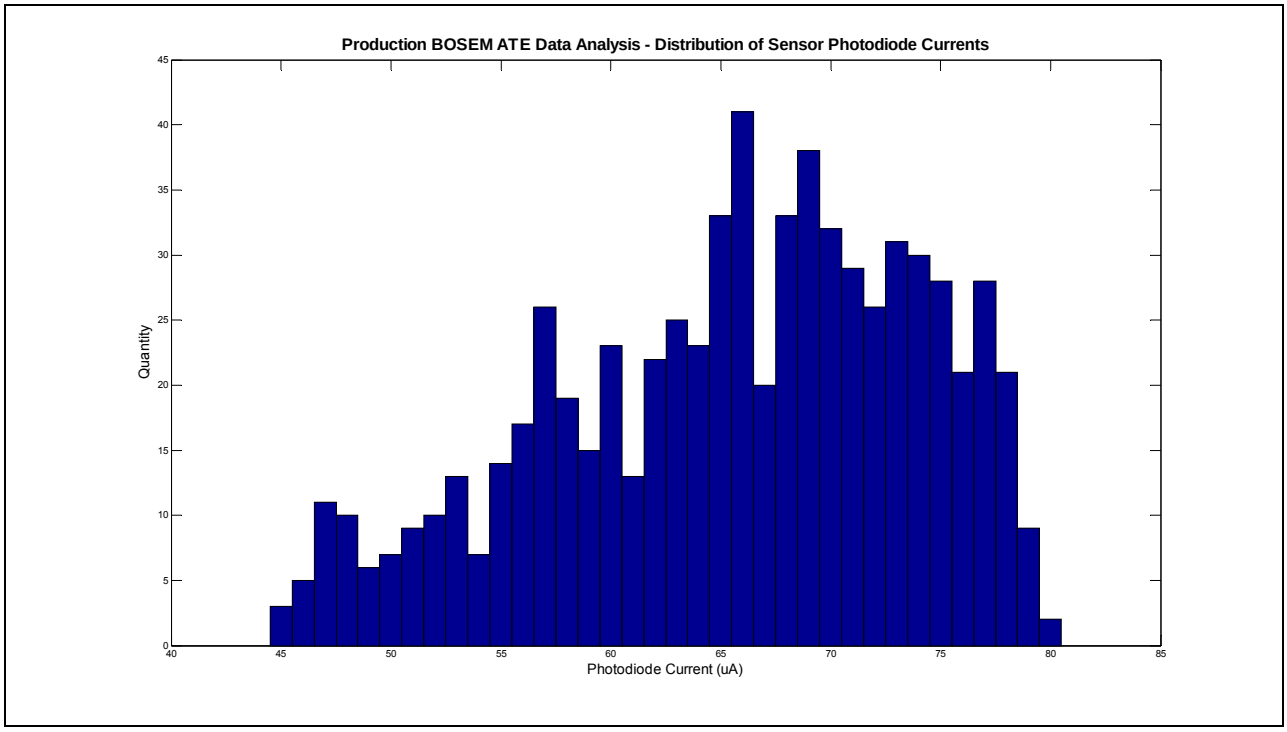

Figure 53. Production BOSEM ATE Data Analysis - Distribution of Sensor Photodiode Currents.

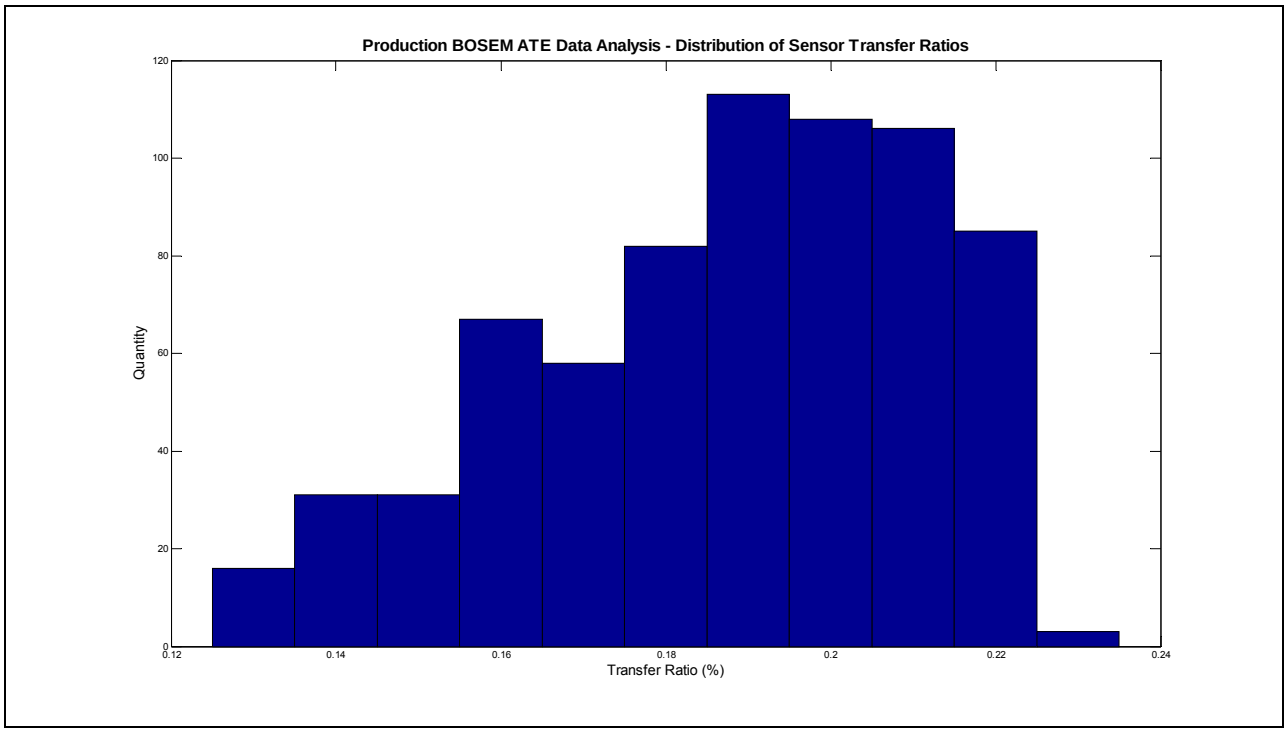

Figure 54. Production BOSEM ATE Data Analysis - Distribution of Sensor Transfer Ratios.

9 APPENDIX A – IRLED Screening Procedure – V3 (UoB Internal)

Preparation Steps

1) Turn OFF lab fluorescent lights, low-voltage halogen lights can be left ON

2) Other non-essential lab equipment should be turned OFF (soldering irons etc)

3) Turn ON Power Supply Unit (Farnell – LT30-2)
   a) Use middle switch (for both ±17V rails)
   b) Observe single red light (middle) illuminate on PSU
   c) Observe three green lights illuminate on Satellite Box

4) Turn ON Low-Noise Preamplifier (Stanford Research Systems – SR560)

5) Conduct visual check that settings are indicated as follows:-
   Filter Cutoffs (Hz) = **DC,** Coupling = **AC,** Source = **A-B,**
   Gain Mode = **Low-Noise,** Gain = **1,** Power = **Line**

6) Turn ON Dynamic Signal Analyzer (Agilent – 35670A)
   a) Wait for unit to complete booting
   b) Insert floppy disk into drive
   c) Select "**Recall/Recall State**" ensure "**Stat1.sta**" selected and press "**Enter**"

7) Turn ON DVM (Beckman – T120B)
   a) Ensure set for **20V DC** range

8) Connect BNC cable between LNP (50Ω output) and DSA (channel 1 input)

Screening Steps

9) Select a Vishay TSTS7100 IRLED device at random from bucket/bag

10) Conduct visual inspection of device batch number (should be from batch #001)

11) Install IRLED into screening jig Teflon mount, with legs protruding from rear

12) Connect IRLED to power lead ensuring polarity is correct as follows:-

a) Tab should be in 7-8 o'clock orientation

b) Positive / anode (red lead) should be on the left

c) Correct polarity confirmed by observing red light (A) on Satellite box go-out

13) Slowly translate the photodiode carrier along the mount towards the IRLED

14) Observe the reading on the DVM and stop at 'peak' voltage. Ensure it's not saturated at 13.5V, if it is then back voltage off to ~12.9V. If peak voltage is below **10.0V** then reject IRLED.

15) Use a fixing screw to lock the photodiode at this peak position

16) Cover the entire assembly with the aluminum foil box (for shielding)

17) Ensure the Low-Noise Preamplifier is not over-ranged (if so then wait)

18) Ensure the Dynamic Signal Analyzer is not over-ranged (if so then wait)

19) Press "Start" button on Dynamic Signal Analyzer

20) Wait while measurements are taken (nominally 10 averages take ~100 seconds)

21) When "averaging complete" read marker value at **10Hz**

a) if **-110dB or lower** then **PASS**, otherwise **FAIL**

22) For devices that pass, save trace to floppy disk, Select **"Save/Save Data/Save Trace/Into File"** ensure "**Trac#.txt**" selected and press **"Enter".** Remove IRLED from screening jig and place in burn-in jig

23) Fail devices, remove IRLED from screening jig and put in "Failed" bin do not save trace

24) Repeat screening procedure for number of IRLEDs required

25) When complete, to shut-down equipment safely, reverse preparation steps 1-7